

1 **Determining the threshold of issuing flash flood**  
2 **warnings based on people's response process**  
3 **simulation**

4  
5 Ruikang Zhang <sup>a, b</sup>, Dedi Liu <sup>a, b, c\*</sup>, Lihua Xiong <sup>a, b</sup>, Jie Chen <sup>a, b</sup>, Hua Chen <sup>a, b</sup>, Jiabo  
6 Yin <sup>a, b</sup>

7  
8 <sup>a</sup> State Key Laboratory of Water Resources Engineering and Management, Wuhan University,  
9 Wuhan, China

10 <sup>b</sup> Hubei Provincial Key Lab of Water System Science for Sponge City Construction, Wuhan  
11 University, Wuhan, China

12 <sup>c</sup> Department of Earth Science, University of the Western Cape, Robert Sobukwe Road,  
13 Bellville 7535, Republic of South Africa

14

15 \* Correspondence to Dedi Liu: [dediliu@whu.edu.cn](mailto:dediliu@whu.edu.cn)

16

17 **Abstract:** The effectiveness of flash flood warnings depends on the people's response  
18 processes to the warnings. And false warnings and missed events cause the people's  
19 negative responses. It is crucial to find a way to determine the threshold of issuing the  
20 warnings that reduces the false warning ratio and the missed event ratio, especially for  
21 uncertain flash flood forecasting. However, most studies determine the warning  
22 threshold based on the natural processes of flash floods rather than the social processes  
23 of warning responses. Therefore, an agent-based model (ABM) was proposed to  
24 simulate the people's response processes to the warnings. And a simulation chain of  
25 "rainstorm probability forecasting - decision on issuing warnings - warning response  
26 processes" was conducted to determine the warning threshold based on the ABM. Liulin  
27 Town in China was selected as a case study to demonstrate the proposed method. The  
28 results show that the optimal warning threshold decreases as the forecasting accuracy  
29 increases. And as the forecasting variance or the variance of the forecasting variance  
30 increases, the optimal warning threshold decreases (increases) for low (high)  
31 forecasting accuracy. Adjusting the warning threshold according to the people's  
32 tolerance levels of the failed warnings can improve warning effectiveness, but the  
33 prerequisite is to increase the forecasting accuracy and decrease the forecasting  
34 variance. The proposed method provides valuable insights into the determination of  
35 warning threshold for improving the effectiveness of flash flood warnings.

36 **Keywords:** Threshold of issuing warnings; Flash flood warnings; People's response  
37 processes; Evacuation; Agent-based model

## 38 **1. Introduction**

39 With the intensification of climate change and human activities (Slater et al., 2021),  
40 flash floods have become one of the most serious disasters threatening economic and  
41 social security (Borga et al., 2019). Flash flood warning has been taken as an effective  
42 and economical means of preventing flash flood disasters (Yin et al., 2023). By issuing  
43 warnings before the occurrence of flash floods, people are advised to or ordered to  
44 evacuate for reducing the casualties. However, the people's responses to the warnings  
45 are complex processes including receiving the warnings, understanding the warnings,  
46 trusting the warnings, and personalizing the flood risk (Mileti, 1995; Parker et al., 2009).  
47 And these complex processes might hinder the evacuation and undermine the  
48 effectiveness of the warnings (Cools et al., 2016). To improve the effectiveness of flash  
49 flood warnings, extensive studies have been done to pursue higher accuracy and longer  
50 lead time of flash flood forecasting (Han and Coulibaly, 2017; Lei et al., 2018).  
51 Unfortunately, the people's responses to the warnings have rarely been explored and  
52 have become a bottleneck in improving the effectiveness of the warnings and reducing  
53 casualties (Bodoque et al., 2019; Wang et al., 2022).

54 The people's negative responses to the warnings have been mainly attributed to the  
55 uncertainties of the flash flood forecasting and the warnings. The uncertainties of flash  
56 flood forecasting are from the uncertainties of meteorological forecasting, observation  
57 data, initial conditions, hydrological and hydraulic model structure, model parameters,  
58 and so on (Boelee et al., 2019). To describe the uncertainties of flood forecasting, a  
59 probabilistic flood forecasting was proposed and had been widely applied in the issuing  
60 warnings by the disaster prevention administrators (Krzysztofowicz, 2001). If the  
61 probability of flash flood disasters from the probabilistic flood forecasting exceeds a  
62 preset threshold, the procedure of the issuing warning will be triggered (Coccia and  
63 Todini, 2011; Todini, 2017). If the threshold is set low, even a low forecasted  
64 probability of flash flood disasters can exceed the threshold, and lots of warnings with  
65 only the low probability of flash flood disaster will be issued, resulting in an increase  
66 in the false warning ratio. In contrast, if the threshold is set high, only the flash flood  
67 disasters with high forecasted probability can be warned, and some flash flood disasters  
68 with not low probability will be missed, leading to an increase in the missed event ratio  
69 (Potter et al., 2021). These two increases from both the false warning ratio and the  
70 missed event ratio can decrease the people's responses to the warnings and expand the

71 casualties. Simmons and Sutter (2009) conducted a statistical analysis of tornado data  
72 from 1986 to 2004, and they found that tornadoes with a higher false warning ratio  
73 killed and injured more people. LeClerc and Joslyn (2015) explored the cry wolf effect  
74 in weather-related decision making through a controlled experimental approach. And  
75 their experiments revealed that the decreasing false warning ratio could increase  
76 people's trust in the warnings when the trust level was in the medium range, while both  
77 too high and too low false warning ratios led to inferior decision making. Ripberger et  
78 al. (2015) found that the false warning ratio and the missed event ratio significantly  
79 reduced people's trust in the National Weather Service, and suppressed their positive  
80 responses via a large regional survey. However, it is impossible to simultaneously  
81 reduce the false warning ratio and the missed event ratio at a certain level of forecasting,  
82 as there is a trade-off between these two ratios as described above. Therefore, it is  
83 crucial to find a way to determine an appropriate threshold that balances the false  
84 warning ratio and the missed event ratio for improving the positive warning responses  
85 and reducing the disaster casualties.

86 Extensive methods have been proposed to determine the threshold of issuing flood  
87 warnings for balancing the false warning ratio and the missed event ratio (Duc Anh et  
88 al., 2020; Ke et al., 2020; Ramos Filho et al., 2021; Tekeli and Fouli, 2017; Young et  
89 al., 2021). The methods have gradually evolved from fixed threshold determination  
90 methods to dynamic threshold determination methods, and from data-driven methods  
91 to simulation-based methods (Cheng, 2013). However, these methods only determined  
92 the threshold of issuing warnings based on the natural processes of flash floods, while  
93 ignoring the social processes of warning responses. The goal of flash flood warnings is  
94 to stimulate the people's responses to the warnings for reducing casualties. Even a  
95 reliable warning cannot be effective without people's positive responses to it. To our  
96 best knowledge, there are very few methods to determine the threshold based on  
97 people's response process simulation. Roulston and Smith (2004) generalized the  
98 warning release into an improved classical binary cost-loss problem, where the people's  
99 warning response level was expressed as a function of false warning ratio, and this  
100 warning response level variable was included in the cost-loss analysis. And the  
101 threshold of issuing warnings was derived with the goal of minimizing the cost loss  
102 ratio under different scenarios. Sawada et al. (2022) proposed a stylized model that  
103 coupled natural and social systems to determine the threshold of issuing warnings. In  
104 this stylized model, the warning response level was attributed to be influenced by both

105 the success rate of the warning and the flood experience, and then was mapped to flood  
106 losses through an empirical equation. However, these studies only described the  
107 warning response level through empirical equations or conceptual models, instead of  
108 describing the warning response processes through process-based models. To reflect  
109 the characteristics of flash flood disaster prevention and the flash flood warning  
110 responses, it is necessary to simulate the people's response processes of receiving  
111 warnings, making evacuation decisions, implementing evacuation, and being  
112 submerged by flash floods (or reaching shelters).

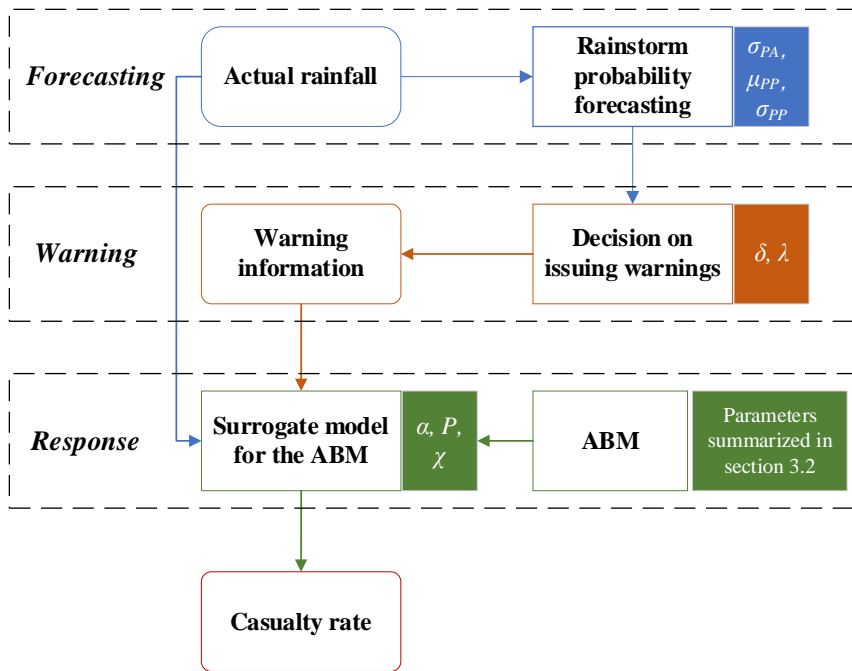
113 Agent-based model (ABM) is a modeling framework for complex systems by  
114 simulating the dynamic interactions between automatic decision-making agents and  
115 between these agents and the environment in a distributed micro level (Janssen and  
116 Ostrom, 2006). As the warning responses are related to a learning process, and also to  
117 personal flood experience and risk perception, ABM is suitable for understanding the  
118 dynamic processes through simulating the individual decision-making (Anshuka et al.,  
119 2022). Additionally, ABM can describe the spatially explicit social-hydrological  
120 processes, such as the dissemination of warning information, the selection of  
121 evacuation routes, and the distribution of flash flood inundation (Sivapalan and  
122 Bloeschl, 2015). Thus, ABM is an effective tool for simulating the people's response  
123 processes to flash flood warnings (Du et al., 2017; [Du et al., 2023](#); Yang et al., 2018;  
124 Zhuo and Han, 2020).

125 The ~~aim~~objective of this study ~~is to propose~~ includes two parts. Firstly, to  
126 simulate people's response processes to flash flood warnings and reveal the impact of  
127 the warning information weight given by people on the effectiveness of warnings, this  
128 study aims to develop a method for determiningprocess-based ABM that combines  
129 natural and social processes (section 2.1). Secondly, to determine the threshold of  
130 issuing warnings (called warning threshold hereafter) based on the ~~people's response~~  
131 ~~process simulation. A process-based ABM is developed to simulate people's response~~  
132 ~~processes to flash flood warnings (section 2.1). A social processes of warning responses,~~  
133 this study attempts to propose a simulation chain of "rainstorm probability forecasting  
134 - decision on issuing warnings - warning response processes" ~~is conducted to determine~~  
135 ~~the warning threshold based on the ABM (section 2.2).~~based on the ABM (section 2.2).  
136 Through the proposed simulation framework for determining the warning threshold, we  
137 will examine the uncertainties in flash flood forecasting that affect the determination of  
138 warning thresholds and the joint impact of forecasting skills and people's tolerance

139 levels of failed warnings on the warning threshold determination. Liulin Town in China  
 140 is selected as a case study to demonstrate the proposed method, and to provide valuable  
 141 insights into the determination of warning threshold for improving the effectiveness of  
 142 flash flood warnings.

143 **2. Methodology**

144 A modeling framework is proposed to determine the warning threshold based on  
 145 people’s response processes. The modeling framework includes the development of an  
 146 ABM and its surrogate model for simulating the people’s response processes to flash  
 147 flood warnings and a chain simulation of “forecasting – warning - response” (see  
 148 Figure 1). First, rainstorm probability forecasting is performed according to actual  
 149 rainfall. And then the warning administrators make decisions to issue warnings based  
 150 on the rainstorm probability forecasting and warning thresholds. If it is decided to issue  
 151 warnings, the warning information and the actual rainfall jointly drive the surrogate  
 152 model of ABM to simulate the people’s response processes. Finally, the casualty rate is  
 153 estimated and the warning threshold that minimizes the casualty rate can be determined  
 154 based on the proposed modeling framework.



155  
 156 **Figure 1.** The proposed modeling framework for determining the warning threshold

157 based on people's response processes (the parameters in a simulation step are indicated  
158 by a rectangular box with the corresponding color background)

## 159 **2.1. An ABM development for simulating people's response** 160 **processes to flash flood warnings**

161 To simulate the people's response processes to flash flood warnings (i.e., including  
162 the receiving warnings, the making evacuation decisions, the implementing evacuation,  
163 and the being submerged by flash floods/the reaching shelters), an ABM is developed  
164 by coupling social and natural sub-systems.

### 165 **2.1.1. Agents and their environments in the ABM**

166 There are two types of agents in the ABM: resident and authority. The resident  
167 agents refer to the people threatened by flash floods. After receiving flash flood  
168 warnings, the agents will decide whether and when to evacuate. If they decide to  
169 evacuate, they will move along the roads towards the shelters. After issuing the  
170 warnings, the flash flood will occur and might wash away the agents who have not  
171 successfully arrived at shelters. The probability of casualties can be estimated based on  
172 the velocity and the depth of the flash flood. The authority agents represent the local  
173 authorities that mandate to prevent the flash flood disasters.

174 The environment in the ABM are the residences, road networks, shelters, and  
175 floodwater. The residence agents are initially randomly distributed in the residences.  
176 The resident agents who have decided to evacuate will move along the road network  
177 instead of freely moving within the ABM area. The shelters are the destinations for  
178 evacuation. The flash flood water not only affects the evacuation decisions and  
179 behaviors of the resident agents but also causes casualties to the resident agents.

### 180 **2.1.2. Sub-modules of the ABM**

181 *Early warning sub-module.* Early warning sub-module simulates the process of  
182 issuing warnings. Owing to the uncertainties of flash flood forecasting, there are  
183 multiple stages of warning in a warning system. Rainstorm red, ready-to-evacuate, and  
184 immediate-evacuation warnings are successively issued in the ABM. The times of  
185 issuing these three warnings are determined by three parameters: lead time of rainstorm  
186 red warning (indicated as ~~lead-time-w1~~ lead-time - w1), ready-to-evacuate warning  
187 (indicated as ~~lead-time-w2~~ lead-time - w2), and immediate-evacuation warning  
188 (indicated as ~~lead-time-w3~~ lead-time - w3).

189 *Social sub-module.* Social sub-module simulates the people's psychological and

190 behavioral response processes to the warnings. The  $j$ -th agent<sup>1</sup> will decide to  
 191 evacuate when his/her overall evacuation intention ( $S_j \in [0, 3]$ ) exceeds a threshold,  $\tau$ , or the water depth near him/her exceeds a threshold,  $EDT$ .  
 192  $EDT$ . There are two components in  $S_j$ : evacuation intention arising from receiving  
 193 warnings ( $S_j^W \in \{1, 2, 3\}$ ), and evacuation intention arising  
 194 from observing neighbors ( $S_j^N \in [0, 1]$ ). The value of  $S_j^W$   
 195 is related to the socio-demographic and socio-psychological attributes of the  $j$ -th  
 196 agent ( $SSC_j$ ) and the stages of the receiving warning from the early warning sub-  
 197 module ( $WT$ ). The relationship can be described by a random forest algorithm. The  
 198 value of  $S_j^N$  equals to the proportion of the  $j$ -th agent's neighbors who have  
 199 decided to evacuate. The weights of the influence of  $S_j^W$  and  $S_j^N$  on the  $S_j$   
 200 are represented by parameters  $\alpha_j$  and  $\beta_j$ , respectively, and  $\alpha_j + \beta_j = 1$ .  
 201 Finally, the overall evacuation intention of the  $j$ -th agent at time  $t$ ,  
 202  $S_{j,t}$ , is a linear combination of overall evacuation intention at time  $t-1$  ( $S_{j,t-1}$ )  
 203 and current information. Learning rate,  $\theta_j$ , measures the weight given  
 204 by the  $j$ -th agent to the obtained information at the current time. If the  $j$ -th agent  
 205 has decided to evacuate, he/she will walk along the shortest road network to the shelters.  
 206 His/her walking speed is estimated by the spatial-grid evacuation model (SGEM) that  
 207 has been developed by the City University of Hong Kong and Wuhan University (Lo et  
 208 al., 2004).

210 *Flood sub-module.* As flash flood can affect the people's evacuation behaviors and  
 211 cause casualties, the flash flood process is simulated in the flood sub-module. The  
 212 Hydrologic Engineering Center's River Analysis System (HEC-RAS) software is  
 213 gaining popularity due to its capabilities to simulate unsteady flow efficiently, and  
 214 identify and visualize flood-prone areas (Hicks and Peacock, 2005; Maidment, 2017).  
 215 The HEC-RAS model has been applied for flood forecasting and warning (Oleyiblo

<sup>1</sup> The agent refers to the resident agent by default



216 and Li, 2010). And it has been adopted in our flood sub-module. The river geometries  
217 such as centerlines, bank lines, and cross-sectional lines are the major parameters  
218 proceeded in the HEC-RAS model to generate flood-prone areas. The spatiotemporal  
219 changes in the depth and velocity of flash floods are simulated by the HEC-RAS model  
220 after the warnings.

### 221 2.1.3. Casualty rate estimation module

222 Current studies generally estimate flood casualties through two types of  
223 influencing factors: environmental factors, and victim characteristics (Petrucci, 2022).  
224 The first type includes the hazard conditions (measured by flood depth and velocity)  
225 and the location and environments where the hazard occurs (e.g., urban/rural,  
226 indoor/outdoor, and distance from floods). Flood velocity and depth are influenced by  
227 underlying surface conditions, such as the topography of flood plains, watershed size,  
228 and land use (Creutin et al., 2009; Penning-Rowsell et al., 2005; Spitalar et al., 2014).  
229 Rural residents are more vulnerable to floods due to the lack of advanced emergency  
230 response systems and forecasting and warning capabilities. The concentration of urban  
231 population and the increase in impermeable surfaces will amplify the flood risk  
232 (Brazdova and Riha, 2014; Terti et al., 2017). The second type includes the attributes  
233 of people (e.g., age, gender, weight, and height), the status of the residence, and whether  
234 the victim has taken adaptive or emergency measures (Papagiannaki et al., 2022;  
235 Petrucci et al., 2019; Petrucci, 2022; Salvati et al., 2018).

236 Takahashi et al. (1992) established a connection between the characterization of  
237 human stability (safe or fall) and flow features such as depth ( $h$ ) and velocity ( $u$ )  
238 through a casualty experiment. If variable  $z$  is set to the linear addition of  $h$  and  $u$   
239 (i.e.,  $z = \beta_0 + \beta_1 \times h + \beta_2 \times u$ ), a logistic regression equation can be used to fit the  
240 relationship between the characterization of human stability (if the person falls, its value  
241 is one, otherwise it is zero) and  $z$ . Based on the experiment data, the parameters ( $\beta_0$ ,  
242  $\beta_1$ , and  $\beta_2$ ) can be estimated, and the logistic regression equation will be used to  
243 predict the probability of casualty by depth and velocity. Based on the spatiotemporal  
244 distribution of the people outputted from the social sub-module and the spatiotemporal  
245 distribution of floodwater outputted from the flood sub-module, the casualty probability  
246 of an agent can be estimated via ~~a~~the logistic regression equation as follows:

247 
$$f(z) = \frac{1}{1 + e^{15.48-z}} \quad f(z) = \frac{1}{1 + e^{15.48-z}} \quad (1)$$

248 where  $z = \beta_0 + \beta_1 \times h + \beta_2 \times u$ ,  $\beta_0 = 12.37$ ,  $\beta_1 = 22.036$ ,  $\beta_2 = 11.517$   
 249  $z = \beta_0 + \beta_1 \times h + \beta_2 \times u$ ,  $\beta_0 = -12.37$ ,  $\beta_1 = 22.036$ ,  $\beta_2 = 11.517$ . The flood water  
 250 depth is represented by  $h$  ( $h \in [0.28, 0.85]$  (m)), and the  
 251 flood water velocity is denoted by  $u$  ( $u \in [0.50, 2.00]$  (m/s))  
 252 ( $u \in [0.50, 2.00]$  (m/s)). The  $j$ -th agent is taken as casualty if the  $h$  exceeds  
 253 0.85 m or  $u$  exceeds 2.00 m/s around him/her. The casualty rate is estimated as the  
 254 proportion of the casualties. A detail description of the ABM can be retrieved from  
 255 Zhang et al. (2024)

256 **2.1.4. A surrogate model development for the ABM**

257 Due to the complexity of the ABM, running this model once requires a significant  
 258 amount of time (Confalonieri et al., 2010). To simulate multiple flash flood events, it is  
 259 necessary to improve the computational efficiency of the ABM. Thus, a Bayesian  
 260 method developed by Oakley and O'Hagan (2004) is used to develop a Gaussian  
 261 process (GP) emulation as a surrogate model of the ABM. The GP emulation can  
 262 simulate the warning response processes more efficiently than the original ABM  
 263 (O'Hagan, 2006). In general, the GP emulation can be represented by an equation:  
 264  $D = f_{GP}(\mathbf{x})$  where  $D$  is the casualty rate at the end of the simulation  
 265 and  $\mathbf{x}$  are a set of parameters of the ABM.

266 A global sensitivity analysis of the ABM reveals that the weight of warning  
 267 influence,  $\alpha$ , is the most sensitive parameter for the casualty rate (Zhang et al.,  
 268 2024). Furthermore, rainfall,  $P$ , is the driving factor causing flash floods. Therefore,  
 269 if there is a flash flood disaster and its corresponding warnings are issued, the ABM can  
 270 be simplified into a two-parameter surrogate model:  $D = f_{GP}^2(\alpha, P)$ . If  
 271 there is a flash flood disaster and no warning is issued, the ABM can be simplified into  
 272 a one-parameter surrogate model:  $D = f_{GP}^1(P)$ .

273 **2.2. Simulation chain of "rainstorm probability forecasting -  
 274 decision on issuing warnings - warning response processes"**

275 **2.2.1. Simulation of the rainstorm probability forecasting**

276 Flash floods often occur if there are sufficient rainstorms in a small basin over a

277 few hours (Collier, 2007; Younis et al., 2008). As the total flood generation and routing  
 278 time is very short, flash flood warnings have to be dependent on the rainstorm  
 279 forecasting for an enough lead time (Zhai et al., 2018). Therefore, the rainstorm  
 280 forecasting determines the flash flood warning decisions. The probabilistic forecasting  
 281 is preferred over the deterministic one as it considers forecasting uncertainties and it is  
 282 beneficial for rational decisions (Krzysztofowicz, 2001). A random probabilistic  
 283 forecasting generator based on Ambühl (2010) is employed to forecast the probability  
 284 distribution of rainfall as follows:

$$285 \quad F \sim N(P + N(\mu_{PA}, \sigma_{PA}^2), N(\mu_{PP}, \sigma_{PP}^2)) \quad (2)$$

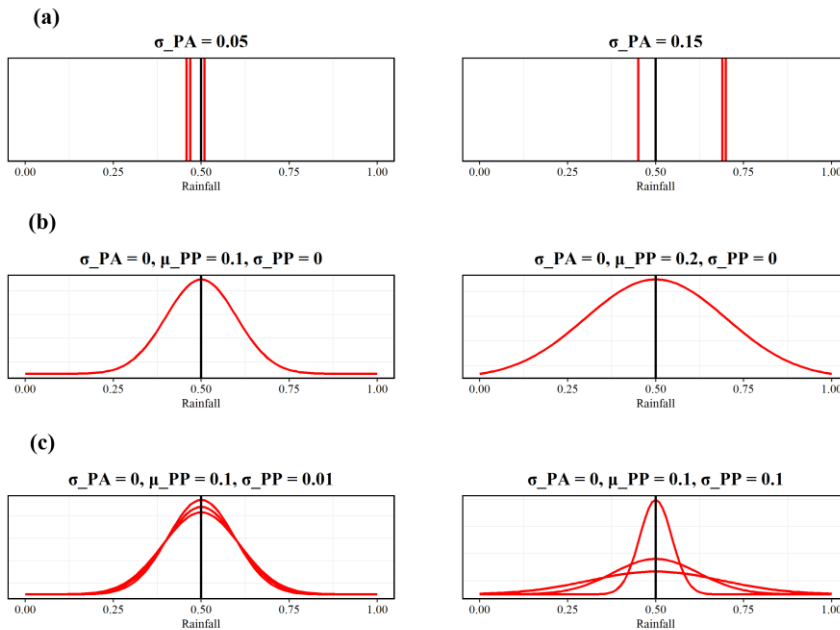
286 where  $F$  is the forecasted rainfall,  $N(\cdot)$  is the Gaussian distribution,  $P$   
 287 is the actual rainfall,  $N(\mu_{PA}, \sigma_{PA}^2)$  reflects the forecasting accuracy, and  
 288  $N(\mu_{PP}, \sigma_{PP}^2)$  reflects the forecasting precision.

289 Although Ambühl (2010) used the gamma distribution to simulate the forecasting  
 290 precision, the Gaussian normal distribution can help improve the interpretability of the  
 291 results. If the probability distribution of forecasted rainfall is assumed to be normal  
 292 distribution and  $\mu_{PA}$  is assumed to be zero according to Sawada et al. (2022), the  
 293 deviation between the median value of forecasted rainfall and the actual rainfall  
 294 (denoted by  $\eta$ ) is determined by  $\sigma_{PA}$ . In other words,  $\eta$  follows a normal  
 295 distribution with a mean of 0 and a variance of  $\sigma_{PA}^2$ . Therefore, there is a positive  
 296 correlation between  $|\eta|$  and  $\sigma_{PA}$ . For example, assuming the actual rainfall is 0.5, if  
 297  $\sigma_{PA} = 0.05$ , the median value of forecasted rainfall from each probability forecast is  
 298 around 0.5. However, if  $\sigma_{PA} = 0.15$ , the median value of forecasted rainfall is likely to  
 299 deviate from 0.5 (see **Figure 2a**). In fact, the probability of  $\eta$  in the interval  $(-3\sigma_{PA},$   
 300  $3\sigma_{PA})$  is 99.73%.

301 Negative  $N(\mu_{PP}, \sigma_{PP}^2)$  is truncated to  $1.0 \times 10^{-6}$  to eliminate the  
 302 negative values of variance. The variance of forecasted rainfall is determined by  $\mu_{PP}$ .  
 303 For example, the probability distribution of forecasted rainfall is relatively concentrated  
 304 if  $\mu_{PP} = 0.1$  while the probability distribution of forecasted rainfall is relatively

带格式的: 缩进: 首行缩进: 2 字符

305 deconcentrated if  $\mu_{PP} = 0.2$  (see Figure 2b). And the variance of the variance of  
 306 forecasted rainfall is determined by  $\sigma_{PP}$ . As shown in Figure 2c, by conducting three  
 307 probability forecasts, there is a similar dispersion degree of probability distributions if  
 308  $\sigma_{PP} = 0.01$  while there is a distinguish dispersion degree of probability distributions if  
 309  $\sigma_{PP} = 0.1$ .  
 310 ~~We set  $\mu_{PA} = 0$  assuming the unbiased forecasting according to Sawada et al.~~  
 311 ~~(2022). If~~ Briefly, if the mean of the  $F$  (i.e.,  $P+N(0, \sigma_{PA}^2)$ ) is taken  
 312 as the forecasting tendency value, the accuracy of the forecasting tendency value will  
 313 be reflected by  $\sigma_{PA}$ . The variance of the  $F$  (i.e.,  $N(\mu_{PP}, \sigma_{PP}^2)$ )  
 314 determines the band-width of the  $F$ . The larger  $N(\mu_{PP}, \sigma_{PP}^2)$ , the  
 315 greater the band-width value of the  $F$ . The variance of the forecasting values is  
 316 determined by  $\mu_{PP}$ , while the variance of the variance of the forecasting values is  
 317 determined by  $\sigma_{PP}$ .



318  
 319 Figure 2. The black line represents the actual rainfall. The value of forecasted rainfall

320 is normalized to 0-1. (a) The median value of forecasted rainfall (represented by the red  
 321 lines) by conducting three probability forecasts under different  $\sigma_{PA}$ . (b) The  
 322 probability distribution of forecasted rainfall (represented by the red line) under  
 323 different  $\mu_{PP}$ . (c) The probability distributions of forecasted rainfall (represented by  
 324 the red lines) by conducting three probability forecasts under different  $\sigma_{PP}$ .

### 325 2.2.2. Simulation of the decision on issuing warnings

326 There is a damage threshold,  $\delta$ . If the  $P$  exceeds this threshold, flash  
 327 flood disasters will occur and cause damages. The probabilistic forecasting system can  
 328 provide the probability that the forecasted rainfall exceeds the  $\delta$  (i.e., the  
 329 probability of flash flood disasters, denoted by  $Prob$ ). If the  $Prob$  is  
 330 larger than a preset threshold,  $\lambda$ , the warning administrators will issue the warnings.  
 331 Thus, the  $\lambda$  is the warning threshold. The warning outcomes are dependent on a  
 332 contingency table (shown in **Table 1**). The outcomes are dependent on two conditions:  
 333 first, whether the  $Prob$  is above the  $\lambda$  or not (i.e., whether to issue warnings  
 334 or not); and second, whether the  $P$  exceeds the  $\delta$  or not (i.e., whether to occur  
 335 a flash flood disaster or not). The interplay of the two conditions leads to four warning  
 336 outcomes: true negative (no warning), false negative (missed event), false positive  
 337 (false warning), and true positive (successful warning). The missed events and the false  
 338 warnings are collectively taken as failed warnings here.

339 **Table 1.** Contingency table defining the warning outcomes <sup>a</sup>

	$P < \delta$ $P < \delta$	$P \geq \delta$ $P \geq \delta$
$Prob < \lambda$	True negative (no warning)	False negative (missed event)
$Prob < \lambda$	0	Damage
$Prob \geq \lambda$	False positive (false warning)	True positive (successful warning)
$Prob \geq \lambda$	Cost	Cost + residual damage

340 <sup>a</sup> Costs and damages associated with each outcome. And they are highlighted in italics.

### 341 2.2.3. Simulation of the warning response processes

342 According to the four warning outcomes in **Table 1**, the warning response  
 343 processes are simulated by the surrogate model of the ABM for estimating the casualty  
 344 rate,  $D$ . If the warning outcome is true negative or false positive, the casualty rate  
 345 is negligible as the actual rainfall,  $P$ , is smaller than the damage threshold,  $\delta$ .  
 346 It should be noted that false positive can cause opportunity cost as there are behavior  
 347 responses to the warnings (i.e., evacuation behaviors). As this study only focuses on the

格式化表格

348 casualty rate, the opportunity cost has been ignored. If the warning outcome is false  
349 negative, there is a flash flood disaster but no warning is issued. In this case, the one-  
350 parameter surrogate model (i.e.,  ~~$D = f_{GP}^1(P)$~~   $D = f_{GP}^1(P)$ ) is employed to simulate the  
351 warning response processes for estimating the casualty rate. If the warning outcome is  
352 true positive, there is a flash flood disaster and its corresponding warnings are issued.  
353 The casualty rate is mitigated by evacuation. The two-parameter surrogate model (i.e.,  
354  ~~$D = f_{GP}^2(\alpha, P)$~~   $D = f_{GP}^2(\alpha, P)$ ) is used to simulate the warning response processes for  
355 estimating the casualty rate. In general, the casualty rate can be described by the  
356 following equation:

$$357 \quad \begin{aligned} \cancel{D} = & \begin{cases} 0 & \text{for true negative or false positive} \\ f_{GP}^1(P) & \text{for false negative} \\ f_{GP}^2(\alpha, P) & \text{for true positive} \end{cases} \\ 358 \quad D = & \begin{cases} 0 & \text{for true negative or false positive} \\ f_{GP}^1(P) & \text{for false negative} \\ f_{GP}^2(\alpha, P) & \text{for true positive} \end{cases} \end{aligned} \quad (3)$$

359 We assume that past warning outcomes affect people's trust levels in the warnings.  
360 Existing studies have found that the recent false warning ratio undermines people's trust  
361 levels in the warnings and their preparedness actions (Jauernic and Van den Broeke,  
362 2017; LeClerc and Joslyn, 2015; Lim et al., 2019; Ripberger et al., 2015). It is  
363 reasonable to assume that people's past experiences with successful (or failed) warnings  
364 increase (or decrease) their trust levels in the warnings. A person's trust level in the  
365 warnings can be described by the parameter  ~~$\alpha$~~   $\alpha$  representing the weight assigned to  
366 the warning information. Therefore,  ~~$\alpha$~~   $\alpha$  after experiencing a flash flood at the  ~~$t$~~   $t$   
367  $t + 1$  time can be described by the following equation:

$$368 \quad \begin{aligned} \cancel{\alpha(t+1)} = & \begin{cases} \alpha(t) & \text{for true negative} \\ \alpha(t) - \chi_{FN} & \text{for false negative} \\ \alpha(t) - \chi_{FP} & \text{for false positive} \\ \alpha(t) + \chi_{TP} & \text{for true positive} \end{cases} \\ 369 \quad \alpha(t+1) = & \begin{cases} \alpha(t) & \text{for true negative} \\ \alpha(t) - \chi_{FN} & \text{for false negative} \\ \alpha(t) - \chi_{FP} & \text{for false positive} \\ \alpha(t) + \chi_{TP} & \text{for true positive} \end{cases} \end{aligned} \quad (4)$$

370 where  $\chi_{FN}$ ,  $\chi_{FP}$ ,  $\chi_{FN}$ ,  $\chi_{FP}$ , and  $\chi_{TP}$ ,  $\chi_{TP}$  are increments of  $\alpha$  for false negative,  
 371 false positive, and true positive, respectively. If  $\alpha$  is larger than one, it is truncated  
 372 to one. If  $\alpha$  is smaller than zero, it is truncated to zero. The people's trust levels in  
 373 the warnings were assumed to be only affected by the past warning outcomes. There  
 374 are other factors (e.g., social education and government authority) that can be  
 375 incorporate into the estimation of the people's trust levels in further research.

#### 376 2.2.4. Performance metrics of the warning

377 Three metrics are used to evaluate the warning performance: the relative casualty  
 378 rate ( $D_r$ ), missed event ratio ( $MER$ ), and false warning ratio ( $FWR$ ).

379 The  $D_r$  is defined as:

$$380 \quad D_r = \frac{D_w}{D_n} \quad (5)$$

381 where  $D_w$  is the average casualty rate of multiple flash floods if there is a flash  
 382 flood warning. And the casualty rate of each flash flood can be estimated by equation  
 383 (3).  $D_n$  is the average casualty rate of multiple flash floods if there is no flash flood  
 384 warning in place (i.e., the casualty rate is dependent only on the natural variability).  
 385 The casualty rate of each flash flood can be estimated by the following equation (6).

$$386 \quad D_n = \begin{cases} 0 & \text{if } P < \delta \\ f_{GP}^1(P) & \text{if } P \geq \delta \end{cases} \quad D_n = \begin{cases} 0 & \text{if } P < \delta \\ f_{GP}^1(P) & \text{if } P \geq \delta \end{cases} \quad (6)$$

387 The lower the value of  $D_r$ , the more effective the flash flood warning is. If the  
 388 objective of flash flood warning is the minimizing the casualties, the optimal warning  
 389 threshold is the threshold where the  $D_r$  is the lowest.

390 Besides  $D_r$ , the  $MER$  and  $FWR$  are used to evaluate the  
 391 performance of the flash flood warning. They are defined by equations (7) and (8):

$$392 \quad MER = \frac{O_{FN}}{O_{TP} + O_{FN}} \quad MER = \frac{O_{FN}}{O_{TP} + O_{FN}} \quad (7)$$

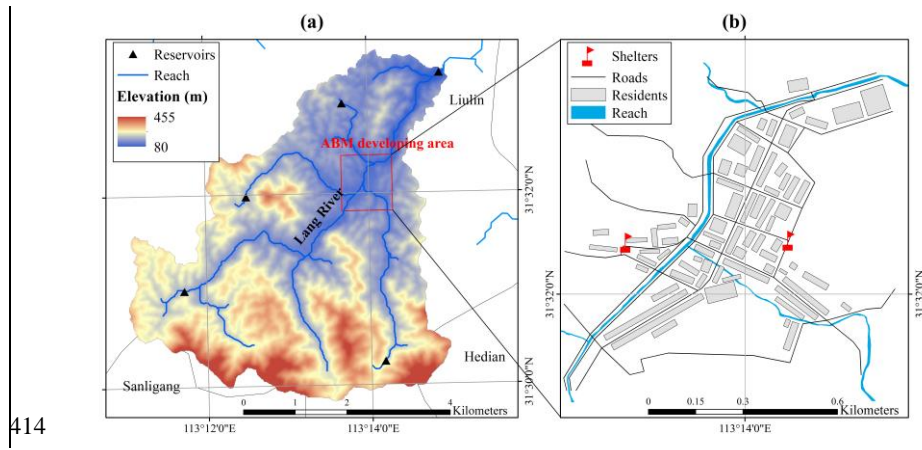
$$393 \quad FWR = \frac{O_{FP}}{O_{FP} + O_{TP}} \quad FWR = \frac{O_{FP}}{O_{FP} + O_{TP}} \quad (8)$$

394 where  $O_{FN}$ ,  $O_{TP}$ ,  $O_{FP}$ ,  $O_{FN}$ ,  $O_{TP}$ ,  $O_{FP}$  are the total number of false negative, true  
 395 positive, and false positive events, respectively.

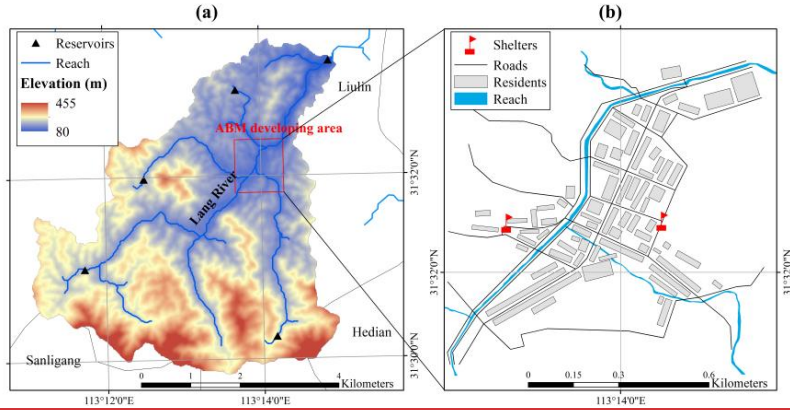
396 **3. Case study**

397 **3.1. Study area**

398 Liulin Town located in Suixian County, Hubei Province, China was selected as  
399 our study area. The Lang River goes through Liulin Town as shown in **Figure 13(a)**  
400 and the red rectangular box indicates the location of the town. The average annual  
401 rainfall is 1,100 mm. Rainfall is unevenly distributed throughout the year, and mainly  
402 concentrates from June to August. The upstream valley of Liulin Town is wider than  
403 that of the downstream. And this river geomorphology hinders flood discharge and  
404 easily causes the flash flood disaster when a rainstormrainfall occurs. Residences in the  
405 town are located on both sides of Langhe River. In the prevention and control map of  
406 flash flood disasters in Suixian County, two communities in Liulin Town are listed as  
407 high-risk and relatively high-risk areas. Especially, an extreme rainstormrainfall with a  
408 volume of 503 mm from 2:00 a.m. to 9:00 a.m. on August 12, 2021 (hereafter called  
409 the 8.12 event) caused a severe flash flood disaster in the town. Unfortunately, 21  
410 people were dead and four people were still missing in this disaster although flash flood  
411 warnings had been issued (Wei, 2021). Exploring the way to determine the threshold  
412 of issuing flash flood warnings in the town will provide valuable information on flash  
413 flood disaster prevention for reducing the casualties.







415  
416 **Figure 13.** Location of the (a) Lang River Basin and (b) Liulin Town

417 **3.2. Setting of the ABM**

418 To set up the environment of the ABM, the residences and road network (see  
 419 **Figure 13**) were imported into the model after processing a digital archive (i.e., World  
 420 Imagery Wayback). To prevent evacuation across the river, two shelters were set up at  
 421 high place on both sides of the Langhe River. And they should not be submerged by  
 422 floods. The parameters of the ABM were set according to calibration, empirical data,  
 423 and related literature (see **Table 2**). The lead ~~times~~ times of the three stages of warning  
 424 and evacuation depth threshold were parameterized from the two-month surveying  
 425 expertise and experience in the study area. The lead time of rainstorm red warning is  
 426 around 180 min in China, and here the lead time was set to 120 min as a conservative  
 427 and unfavorable scenario. As people should immediately move to a shelter after  
 428 receiving an immediate-evacuation warning, the lead time of immediate-evacuation  
 429 warning is related to the travel time of the people to the shelter. The person farthest  
 430 from the shelter needs about 25 min to travel to the shelter, so the lead time of  
 431 immediate-evacuation warning was set to 30 min. According to the lead times of  
 432 rainstorm red warning and immediate-evacuation warning, it was assumed that the lead  
 433 time of ready-to-evacuate warning was between the two, that is, 60 min. The three  
 434 hyperparameters of the random forest model were calibrated by the empirical data from  
 435 our survey. A sampling without replacement was conducted on the empirical data and  
 436 the sample was used to assign the initial ~~SSC~~ SSC values of the agents. The random  
 437 forest model calibration, the survey, and the method of assigning ~~SSC~~ SSC values  
 438 were detailed in Zhang et al. (2024). The values of  ~~$\theta_j$~~   $\theta_j$  and  ~~$p_j$~~   $p_j$  of the  $j$ -th

439 agent were sampled from the Gaussian distributions according to the exiting literature  
 440 (Du et al., 2017).  $S_j = 2$ . The setting of these two parameters aimed to reflect people's  
 441 general behavior.  $\beta_j = 0.5$  represents a general and unbiased behavior that gives same  
 442 weights to current flood information and past opinion on flood risk. And  $p_j = 0.1$   
 443 means flood information being checked every ten minutes.  $S_j = 2$  is set to indicate no  
 444 decision making on evacuation for the  $j$ -th agent in the empirical data while  $S_j > 2$   
 445  $S_j > 2$  means the evacuation decision of the agent. Hence, the value of  $\tau$  was set  
 446 to 2. A global sensitivity analysis has been performed to explore the relative impacts of  
 447 these parameters on the casualty rate and can be retrieved from Zhang et al. (2024).

448

449 **Table 2.** Fixed ABM parameters

Sub-module	Parameters	Symbol	Values	Remark
Early warning	Lead time of rainstorm red warning	<del>lead-time-w1</del> <u>lead-time-w1</u>	120 min	Author estimation <sup>a</sup>
	Lead time of ready-to-evacuate warning	<del>lead-time-w2</del> <u>lead-time-w2</u>	60 min	Author estimation <sup>a</sup>
	Lead time of immediate-evacuation warning	<del>lead-time-w3</del> <u>lead-time-w3</u>	30 min	Author estimation <sup>a</sup>
Random forest	Number of trees	<del>ntree</del> <u>ntree</u>	500	Calibration
	Number of candidate variables	<del>mtry</del> <u>mtry</u>	6/1/6 <sup>b</sup>	Calibration
	Minimum size of nodes	<del>nodesize</del> <u>nodesize</u>	10/1/10 <sup>b</sup>	Calibration
	Socio-demographic and socio-psychological characteristics of resident agents	<del>SSC</del> <u>SSC</u>		Empirical data
Opinion dynamics	Learning rate	<del><math>\theta</math></del> <u><math>\theta</math></u>	0.5 (0.1) <sup>c</sup>	Literature reference (Du et al., 2017)
	Probability of receiving early warnings	<del><math>p</math></del> <u><math>p</math></u>	0.1 (0.1) <sup>c</sup>	Literature reference (Du et al., 2017)
	Evacuation threshold	<del><math>\tau</math></del> <u><math>\tau</math></u>	2	Empirical data
Others	Visual range	<del>VR</del> <u>VR</u>	40 m	Literature reference (Wu et al., 2022)
	Evacuation threshold depth	<del>EDT</del> <u>EDT</u>	0.28 m	Author estimation <sup>a</sup>

设置了格式: 字体: Times New Roman, 小四

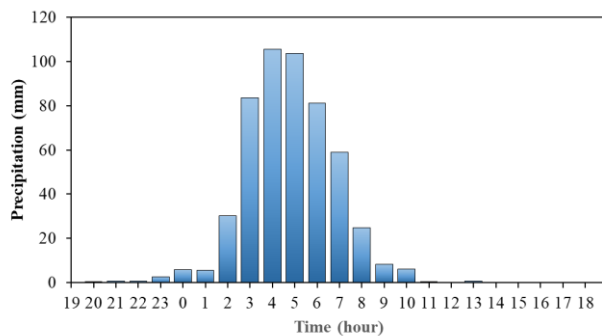
带格式的: 题注

格式化表格

格式化表格

450 <sup>a</sup> These estimations are from the two-month surveying expertise and experience of the authors  
451 in the study area. <sup>b</sup>  $x_1/x_2/x_3$  indicates the values of the factors are  $x_1$ ,  $x_2$ , and  $x_3$  for the rainstorm  
452 red, the ready-to-evacuate, and the immediate-evacuation warnings, respectively. <sup>c</sup>  $x_1$  ( $x_2$ )  
453 indicates the values of the factors are sampled from a normal distribution with mean value of  
454  $x_1$  and variance of  $x_2$

455 The flood-module of the ABM was formed by a two-dimensional (2D)  
456 hydrodynamic model in the Langhe River Basin through HEC-RAS. Terrain  
457 information was obtained from the digital elevation model (DEM) at a spatial resolution  
458 of 12.5 m provided by the Advanced Land Observing Satellite (ALOS). Cells with size  
459 of 30 m were generated within the 2D flow areas. The Manning's coefficient was set to  
460 a unified comprehensive value of 0.045. The upstream boundary condition was set as  
461 the ~~rainstorm~~rainfall process. The hyetograph was selected by the measured rainfall  
462 process of the 8.12 event. Specifically, the hourly rainfall was greater than 30.0 mm  
463 from 2:00 to 7:00 on August 11, 2021 and the 6-h rainfall was up to 462.6 mm (see  
464 **Figure 24**). The 6-h rainfall process was input into the HEC-RAS as the hyetograph.  
465 As Baiguo River reservoir is in the outlet, the downstream boundary condition was set  
466 as the normal water level of the reservoir. The spatiotemporal changes in the depth and  
467 velocity of flash floods were exported after running the model at a temporal interval of  
468 2 min and spatial resolution of 12.5 m. it should be noted that the hyetograph was  
469 selected as the measured rainfall process of the 8.12 event. More uneven hyetographs  
470 should be taken in the flash flood simulation, and the impact of hyetograph on the  
471 warning threshold determination can be explored in further research.



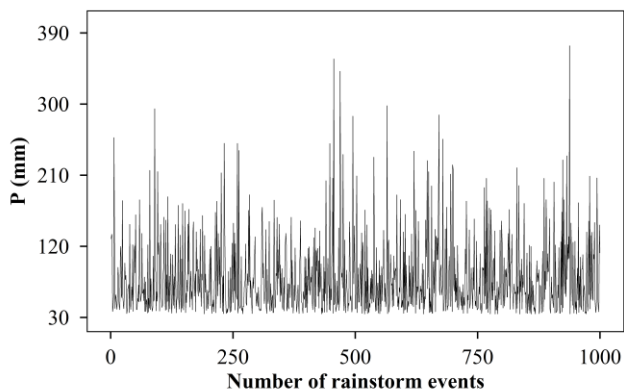
472  
473 **Figure 24.** The rainfall process from 19:00 on August 11 to 19:00 on August 12, 2021  
474 of Liulin Meteorological Station

475 The ABM was run by covering the processes from issuing warnings to flash flood  
476 at a time step of 1 min and spatial resolution of 9.6 m. And 500 agents were assumed  
477 to be involved in the simulations. Due to the inherent randomness of the ABM, the

478 averages of the outputs from the repeating 1,000 times for running the ABM were  
479 obtained to ensure stable outputs.

### 480 3.3. Rainfall data

481 A series of rainfall data was imported into the ABM for simulating a series of  
482 possible flash flood disasters. ~~Synthetic First, synthetic~~ rainfall series ~~are required were~~  
483 ~~generated~~ to ensure the representative of the extreme events. The annual maximum 6-h  
484 rainfall,  ~~$P$~~   $P$ , was assumed to follow the Pearson III distribution. Its values of mean  
485 and  ~~$C_v$~~   $C_v$  in the basin above Liulin Town were estimated to be 80 mm and 0.6,  
486 respectively, according to Atlas of Statistical Parameters of ~~rainstorm~~rainfall in Hubei  
487 Province (2008).  ~~$C_s / C_v$~~   $C_s / C_v$  was taken as 3.5 in Hubei Province. ~~A total of~~ 1,000  
488 synthetic ~~rainstorm~~rainfall events were randomly generated by the Pearson III  
489 distribution, and the result was shown in **Figure 35**. ~~Second, a rainfall event in the~~  
490 ~~synthetic rainfall events was input into the flood module of ABM, and then converted~~  
491 ~~into a flash flood event. According to the flash flood event, the degree of flash flood~~  
492 ~~disaster had been estimated, and people's attitudes towards the corresponding warning~~  
493 ~~had been recorded. The people's attitudes can influence the subsequent warning~~  
494 ~~response processes. Then, the next rainfall event in the synthetic rainfall events was~~  
495 ~~input into the ABM, and the above simulation process was repeated.~~



496

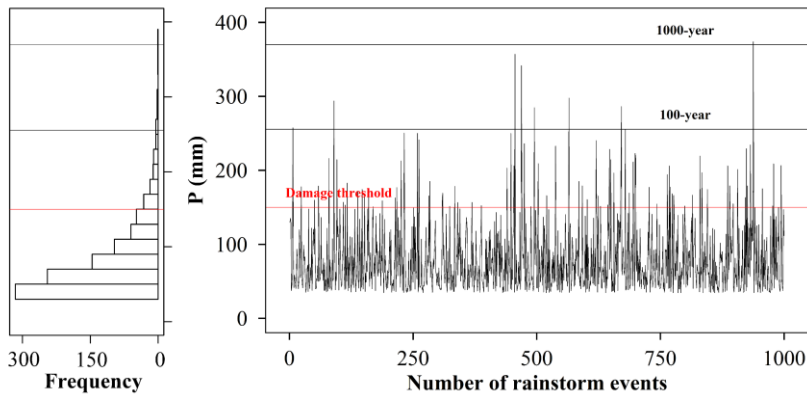


**Figure 35.** 1,000 synthetic series of ~~rainstorm~~rainfall events (right). Histogram statistical results of the synthetic rainfall events. The three horizontal lines from top to bottom represent the rainfall for 1000-year return period, 100-year return period, and triggering disasters, respectively

### 3.4. Model test experiments

~~To determine the warning threshold under different forecasting skills for minimizing the relative casualty rate, three possible values of each of the three parameters (i.e.,  $\sigma_{PA}$ ,  $\mu_{PP}$ , and  $\sigma_{PP}$ )~~ The impact of forecasting skills on the warning threshold determination can be explored by setting different values of  $\sigma_{PA}$ ,  $\mu_{PP}$ , and  $\sigma_{PP}$ . In real-world flood warning scenarios, these three parameters can be estimated by statistical methods, such as moment estimation method and maximum likelihood estimation method. Specifically, the actual rainfall and the corresponding probability forecasting results in the history can be collected under a certain forecasting skill. Each rainstorm event is taken as a sample, and the observed rainfall, the median value of probability forecasted rainfall, and the variance of probability distribution for the rainstorm event are estimated. By collecting multiple rainstorm events, these three parameters can be estimated using statistical methods for a certain forecasting skill. As we aim to examine the uncertainties in flash flood forecasting that affect the determination of warning thresholds in this study, three possible values of each of the three parameters (i.e.,  $\sigma_{PA}$ ,  $\mu_{PP}$ , and  $\sigma_{PP}$ ) were prepared to reflect different forecasting skills (see Table 3) and their interactive effects on the determination of warning threshold were tested.

520 Rainstorm red warning is the highest level of meteorological risk warning in the  
 521 mainland of China. When the rainstorm red warning is issued, floods tend to cause  
 522 damage and the residents in flood risk area are advised to evacuate (Wang et al., 2020).  
 523 If the 6-hour rainfall is up to 150 mm, the rainstorm red warning will be issued  
 524 (Shanghai Meteorological Bureau, 2019). Thus, the value of  $\delta$  was taken as 150  
 525 mm in the case study.

526 **Table 3.** Model test experiment for determining the warning threshold under different  
 527 forecasting skills

Parameters	Symbol	Values
The accuracy of the forecasting tendency value	$\sigma_{PA}$	{0.05, 0.10, 0.15}
The variance of the forecasting values	$\mu_{PP}$	{0.0, 0.1, 0.2}
The variance of the variance of the forecasting values	$\sigma_{PP}$	{0.0, 0.1, 0.2}
Damage threshold	$\delta$	150 mm
Increment of $\alpha$ for false negative	$\chi_{FN}$	0.1
Increment of $\alpha$ for false positive	$\chi_{FP}$	0.1
Increment of $\alpha$ for true positive	$\chi_{TP}$	0.1

格式化表格

528 Besides the uncertainties of the forecasting, there are uncertainties in people's  
 529 response processes to the uncertain forecasting. To determine the warning threshold  
 530 under different forecasting skills and tolerance levels of the failed warnings, the  
 531 warning threshold was determined under different  $\sigma_{PA}$  and combinations of  
 532 parameters related to the increments of  $\alpha$  (i.e.,  $\chi_{FN}$ ,  $\chi_{FP}$ , and  $\chi_{TP}$ )  
 533 through Exp1 in **Table 4**, and under different  $\mu_{PP}$  and combinations of  
 534 parameters related to the increments of  $\alpha$  through Exp 2 in **Table 4**. The higher the  
 535  $\chi_{FN}$  and  $\chi_{FP}$ , the lower the tolerance levels of the people towards the missed  
 536 event and the false warnings, respectively.

537 **Table 4.** Model test experiment for determining the warning threshold under different  
 538 forecasting skills and tolerance levels of the failed warnings

Parameters	Symbol	Values	
		Exp1	Exp2
The accuracy of the forecasting tendency value	$\sigma_{PA}$	{0.05, 0.10, 0.15}	0.075
The variance of the forecasting values	$\mu_{PP}$	0.15	{0.0, 0.1, 0.2}
The variance of the variance of the forecasting values	$\sigma_{PP}$	0.075	0.075

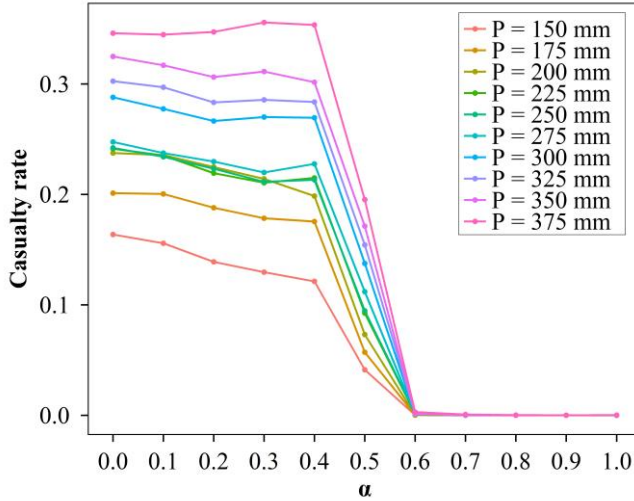
格式化表格

Parameters	Symbol	Values	
		Exp1	Exp2
Damage threshold	$\delta$	150 mm	150 mm
Increments of $\alpha$ for false negative, false positive, and true positive	$\chi_{FN}$ , $\chi_{FP}$ , $\chi_{TP}$	{0.1/0.1/0.1, 0.8/0.8/0.1, 0.8/0.1/0.1, 0.1/0.8/0.1}	{0.1/0.1/0.1, 0.8/0.8/0.1, 0.8/0.1/0.1, 0.1/0.8/0.1}

539 **4. Results and discussions**

540 **4.1. The casualty rate from people’s response process simulation**

541 To determine the warning threshold based on the people’s response process  
542 simulation, the ABM with different values of  $P$  and  $\alpha$  were run to generate  
543 corresponding casualty rates, and these simulations were taken as sample data to train  
544 the GP emulation as a surrogate model of the ABM, as shown in **Figure 46**. And it has  
545 shown the variation of casualty rate with  $\alpha$  under different  $P$ . There are three  
546 stages of change in the casualty rate as  $\alpha$  increases regardless of  $P$ . When  $\alpha$   
547 increases from 0.0 to 0.4, the casualty rate slowly decreases; but as  $\alpha$  continues  
548 to increase to 0.6, the rate of decline becomes faster. When  $\alpha$  is greater than or  
549 equal to 0.6, everyone arrives at the shelters before the flash flood disaster arrives and  
550 there are no casualties regardless of  $P$ . This result implies that it is very important  
551 and effective to enhance people’s trust levels in the warnings when people have similar  
552 trust levels in warning information and their neighbors. When people's trust in warning  
553 information decreases, their evacuation decisions will become more dependent on  
554 whether their neighbors are evacuating or not. In other words, the increase in the overall  
555 evacuation intention ( $S$ ) of agents requires their neighbors to take evacuation actions.  
556 However, taking evacuation actions requires the increase in  $S$  in turn. Thus,  
557 waiting for others’ evacuation ultimately leads to neither an increase in  $S$  nor the  
558 implementation of evacuation actions.



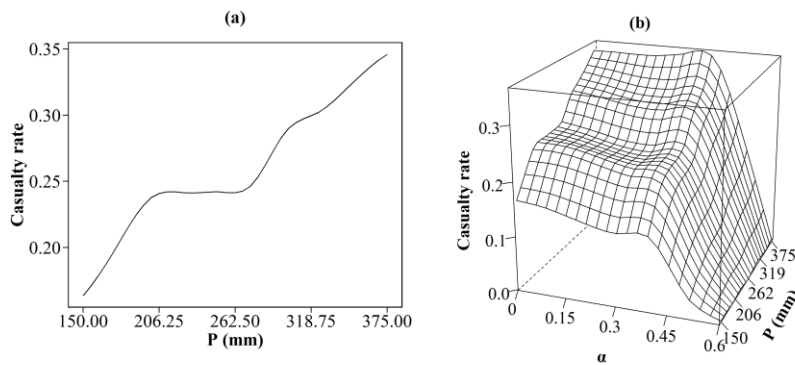
559

560 **Figure 46.** The casualty rate under different values of  $\underline{P}$  and  $\underline{\alpha}$  from ABM  
 561 simulations

562 Because the casualty rate is zero when  $\underline{\alpha}$  is greater than or equal to 0.6  
 563 regardless of  $\underline{P}$ , the one-parameter and two-parameter GP emulations were trained  
 564 for  $\underline{\alpha}$  with a value less than 0.6 and the results were shown in **Figure 57**. The  
 565 training result for one-parameter GP emulation shows that there are also three stages in  
 566 the increase of casualty rate as  $\underline{P}$  increases. When  $\underline{P}$  increases from 150 to  
 567 200 mm, the casualty rate increases; but if  $\underline{P}$  increases from 200 to 260 mm, the  
 568 casualty rate remains almost unchanged. When  $\underline{P}$  exceeds 260 mm and continues  
 569 to increase, the casualty rate starts to increase again. This result indicates that there is  
 570 spatial heterogeneity of flood risk levels in the case study. It is necessary to classify  
 571 flood risk zones and distinguish water level or rainfall thresholds for triggering  
 572 evacuation according to different flood risk levels. The training result for two-parameter  
 573 GP emulation shows the complex responses of casualty rate to changes in  $\underline{\alpha}$  and  
 574  $\underline{P}$ . When  $\underline{\alpha}$  is less than 0.4, there are three stages of changes in the casualty rate  
 575 as  $\underline{P}$  increases. As  $\underline{\alpha}$  increases from 0.4 to 0.6, the relationship between  $\underline{P}$   
 576 and casualty rate tends to be linearly positive, and the difference in casualty rates under  
 577 different  $\underline{P}$  gradually reduces. This result means that the trust level in the warnings  
 578 becomes the dominant factor in determining the casualty rate when the people's trust



579 levels in the warnings and their neighbors are similar (i.e., when the value of  $\alpha$  is  
 580 the range of 0.4 to 0.6).

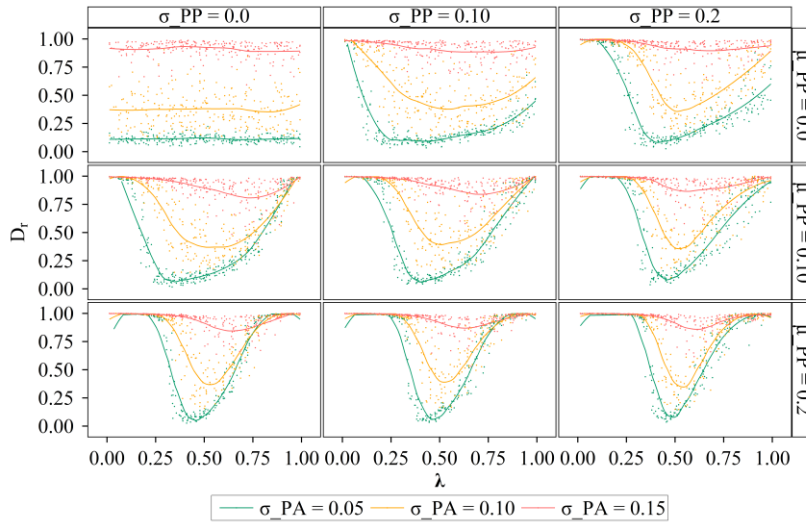


581  
 582 **Figure 57.** Trained (a) one-parameter and (b) two-parameter GP emulations for casualty  
 583 rate

584 **4.2. Determining the warning threshold under different forecasting**  
 585 **skills for minimizing casualties**

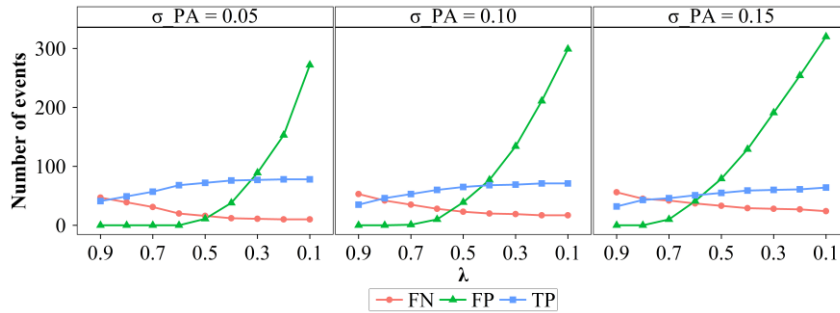
586 To determine the warning threshold under different forecasting skills for  
 587 minimizing casualties, 250-member Monte Carlo simulations were performed on the  
 588 simulation chain of "rainstorm probability forecasting - decision on issuing warnings -  
 589 warning response processes" by randomly perturbing the warning threshold,  $\lambda$ ,  
 590 under different values of parameters controlling the forecasting skills (see **Figure 68**).  
 591 Different rows represent different values of  $\mu_{pp}$ , and there is a larger forecasting  
 592 variance in the sub-graph of the lower row. Similarly, there is a larger variance of the  
 593 forecasting variance in the sub-graph of the right column compared to the sub-graph of  
 594 the left column. The highest forecasting accuracy is represented by the green curves,  
 595 followed by the yellow curves, and finally the red curves. In all the sub-graphs, there is  
 596 the highest relative casualty rate in the red curves, followed by the yellow curves, and  
 597 finally the green curves. Therefore, the lower the forecasting accuracy, the higher the  
 598 relative casualty rate. The optimal warning threshold can be taken as the value of  $\lambda$   
 599 where the relative casualty rate,  $D_r$  is lowest. The optimal warning thresholds are  
 600 the lowest in the green curves, followed by the yellow curves, and finally the red curves  
 601 in all the sub-graphs. Thus, the lower the forecasting accuracy, the higher the optimal

602 warning threshold. The reasons can be found in **Figure 79**. As the warning threshold  
 603 decreases, the number of false warnings and successful warnings increases, and more  
 604 warnings are issued. However, if the forecasting accuracy is low, the proportion of false  
 605 warnings is higher than that of successful warnings among the additional warnings  
 606 issued. For example, as the warning threshold decreases, the green curve for low  
 607 forecasting accuracy rises faster than that for high forecasting accuracy. This means that  
 608 if the forecasting accuracy is low, as the warning threshold decreases, the increase speed  
 609 of false warnings is higher than that of successful warnings. In addition, when the  
 610 warning threshold is less than 0.7, the green curve begins to rise rapidly for  ~~$\sigma_{PA} = 0.15$~~   
 611  $\sigma_{PA} = 0.15$ , while it does not start to rise rapidly until the warning threshold is less than  
 612 0.5 for  ~~$\sigma_{PA} = 0.15$~~   $\sigma_{PA} = 0.15$ . Therefore, when the forecasting accuracy is low, a high  
 613 warning threshold should be set. As the forecasting accuracy increases, lowering the  
 614 warning threshold can result in more successful warnings without significantly  
 615 increasing false warnings, thereby improving the effectiveness of flash flood warnings.



616  
 617 **Figure 68.** The relationship between the relative casual rate,  $D_r$ , and the warning  
 618 threshold,  $\lambda$ , under different values of  $\sigma_{PA}$ ,  $\mu_{PP}$ ,  $\sigma_{PA}$ ,  $\mu_{PP}$ , and  $\sigma_{PP}$ .  
 619 Different rows and columns represent different values of  $\mu_{PP}$  and  $\sigma_{PP}$ ,  
 620 respectively. Different colors represent different values of  $\sigma_{PA}$ . Each dot shows

621 the result of the individual Monte Carlo simulation



622  
 623 **Figure 79.** The changes in the number of false negative, false positive, and true positive  
 624 events as warning threshold decreases,  $\lambda$  under different values of  $\sigma_{PA}$ . The  
 625 range of  $\lambda$  is reversed from 0.9 to 0.1

626 In terms of the impacts of the forecasting variance (see **Figure 68**), there is a larger  
 627 forecasting variance and a higher relative casualty rate of three colored curves in the  
 628 sub-graph of the lower row. Thus, the larger the forecasting variance, the higher the  
 629 relative casualty rate. For the optimal warning threshold, the differences in the optimal  
 630 warning thresholds of these three colored curves are smaller in the sub-graph of the  
 631 lower row. For instance, as the forecasting variance increases, the optimal warning  
 632 thresholds for the red curves decrease while the optimal warning thresholds for the  
 633 green curves increase. This result means that the larger the forecasting variance, the  
 634 lower the optimal warning threshold for low forecasting accuracy, while the larger the  
 635 forecasting variance, the higher the optimal warning threshold for high forecasting  
 636 accuracy. When the forecasting accuracy is at a low level, a large forecasting variance  
 637 is actually beneficial for improving the forecasting skills. High forecasting skill means  
 638 that more successful warnings and fewer false warnings are issued after lowering the  
 639 warning threshold. Therefore, if the forecasting accuracy is at a low level, as the  
 640 forecasting variance increases, the warning threshold can be lowered. On the contrary,  
 641 if the forecasting accuracy is at a high level, as the forecast variance increases,  
 642 increasing the warning threshold can significantly decrease the false warnings and  
 643 improve the effectiveness of flash flood warnings. Finally, we focused on the impacts  
 644 of the variance of the forecasting variance. Similar to the impacts of the forecasting  
 645 variance, the larger the variance of the forecasting variance, the higher the relative  
 646 casualty rate. As the variance of the forecasting variance increases, the optimal warning

647 threshold tends to decrease for low forecasting accuracy or to increase for high  
 648 forecasting accuracy.

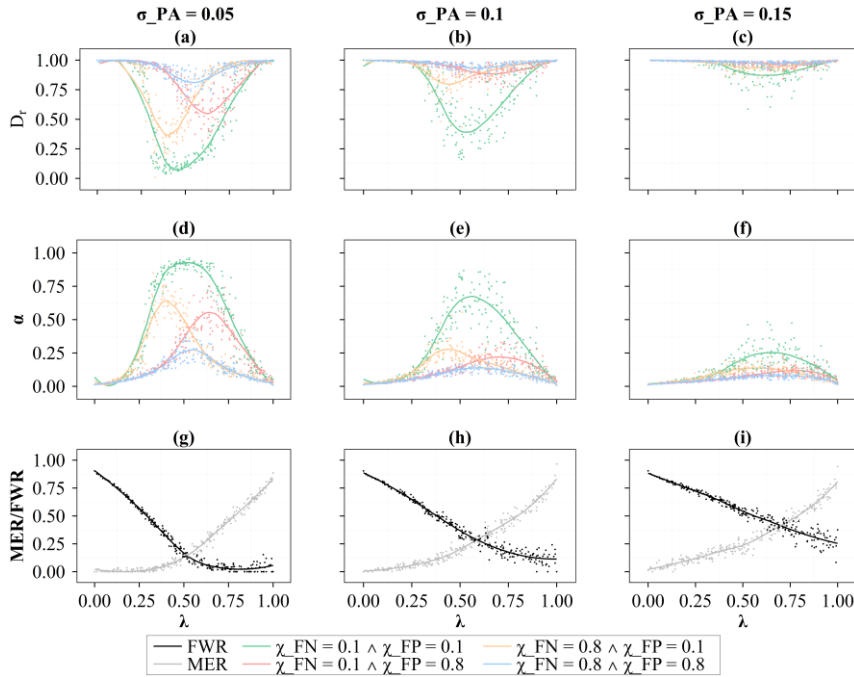
649 The impacts of the three parameters (i.e.,  $\sigma_{PA}$ ,  $\mu_{PP}$ , and  $\sigma_{PP}$ ) on  
 650 the shape of the relationship curve between  $D_r$  and  $\lambda$  can be analyzed as  
 651 follows. As shown in **Figure 6**,  $\sigma_{PA}$  determines the height of the curve, while  
 652  $\mu_{PP}$  and  $\sigma_{PP}$  determine the width of the curve. Specifically, as the  
 653 forecasting accuracy increases, the stationary point of the curve moves down and the  
 654 curve becomes higher; as the forecasting variance or the variance of the forecasting  
 655 variance increases, the curve becomes narrower. If the forecasting accuracy is high and  
 656 the forecasting variance and the variance of the forecasting variance are large, the curve  
 657 will become high and narrow, such as the green curve for  $\mu_{PP} = 0.2$  and  
 658  $\sigma_{PP} = 0.2$ . And there is only a low relative casualty rate near the optimal  
 659 warning threshold in this green curve. Thus, it is more important to determine the  
 660 optimal warning threshold for minimizing casualties if the forecasting accuracy is  
 661 higher, and the forecasting variance and the variance of the forecasting variance are  
 662 larger.

### 663 4.3. Determining the warning threshold under different forecasting 664 skills and tolerance levels of the failed warnings for minimizing 665 casualties

666 To determine the warning threshold under different forecasting skills and tolerance  
 667 levels of the failed warnings for minimizing casualties, the simulation chain of  
 668 "rainstorm probability forecasting - decision on issuing warnings - warning response  
 669 processes" was run with random values of  $\lambda$  under different  $\sigma_{PA}$  and  
 670 combinations of parameters related to the increments of  $\alpha$  (i.e.,  $\chi_{FN}$ ,  $\chi_{FF}$ ,  $\chi_{FN}$ ,  
 671  $\chi_{FP}$ , and  $\chi_{TP}$ ) (see **Figure 810**), and different  $\mu_{PP}$  and combinations of  
 672 parameters related to the increments of  $\alpha$  (i.e.,  $\chi_{FN}$ ,  $\chi_{FF}$ ,  $\chi_{FN}$ ,  $\chi_{FP}$ , and  $\chi_{TP}$ )  
 673 (see **Figure 911**). Owing to the similar roles of  $\mu_{PP}$  and  $\sigma_{PP}$ , the effects of  
 674  $\sigma_{PP}$  on the determination of warning threshold were not explored here. As shown  
 675 in **Figure 810**, the optimal warning thresholds for the yellow curves are the lowest. The

676 yellow curves represent scenarios that people's trust in warnings is sensitive to false  
677 negative events and people have a low tolerance level for the missed events. To reduce  
678 the missed event ratio, the warning threshold should be lowered (see **Figure 8g10g**).  
679 Therefore, the warning threshold should be lowered for increasing people's trust levels  
680 in warnings and reducing casualties if people have a lower tolerance level for the missed  
681 events. Similarly, the warning threshold should be increased if the people's tolerance  
682 levels for the false warnings become lower (see the red curves). And if the people's  
683 tolerance for both the missed events and the false warnings decreases to the same level,  
684 the optimal warning threshold remains almost unchanged, but the relative casualty rate  
685 overall increases (see the blue curves). As for the relative casualty rate, the relative  
686 casualty rates of the yellow curves are lower than those of the red curves. This result  
687 suggests that compared to the missed events, the people's low tolerance levels for the  
688 false warnings are less conducive to the effectiveness of flash flood warnings. As shown  
689 in **Figure 79**, the number of false warnings is greater than the number of missed events  
690 in general. Therefore, if the people's tolerance levels for the false warnings is low, their  
691 trust levels in warnings are more likely to decrease, leading to the effects of "cry wolf".

692 By comparing **Figure 8a10a** and **Figure 8b10b**, the overall height of the curves  
693 decreases when the forecasting accuracy decreases, as discussed in the last paragraph  
694 of section 4.2. However, compared to green curve, the heights of other curves decrease  
695 more significantly. And the relative casualty rates are high at any warning threshold  
696 (i.e.,  $D_r > 0.75$ ,  $D_r > 0.75$ ) except for the green curve when the  $\sigma_{PA} \sigma_{PA}$  increases  
697 from 0.05 to 0.1. It is more pronounced when the  $\sigma_{PA} \sigma_{PA}$  further increases to 0.15.  
698 Therefore, as the forecasting accuracy decreases, the benefits gained by adjusting the  
699 warning threshold based on the people's tolerance levels of the failed warnings  
700 decreases. In other words, no matter how the warning threshold is adjusted, the relative  
701 casualty rate is high and the effectiveness of warning is at a low level.

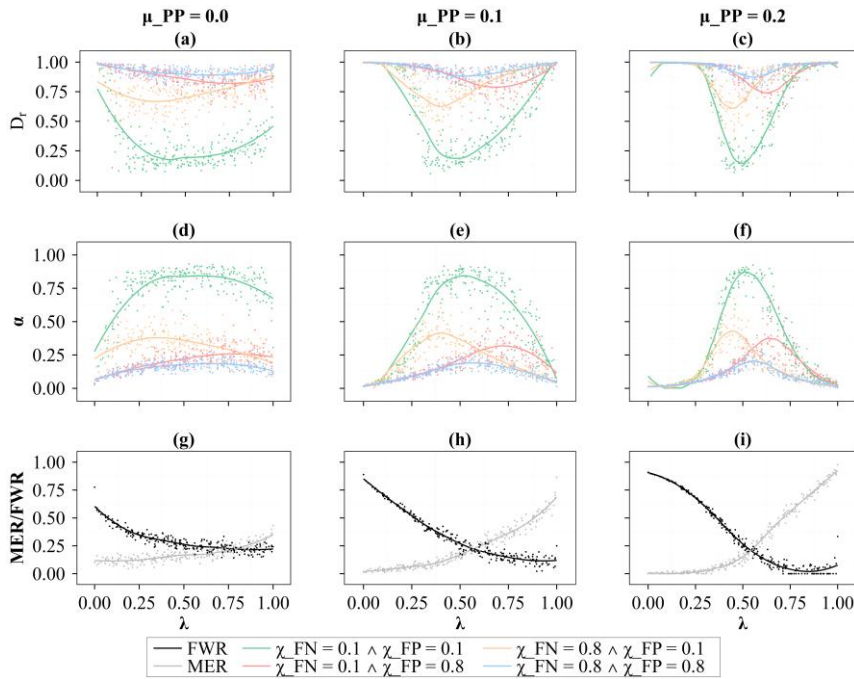


702  
703 **Figure 810.** (a-c) The relationship between the warning threshold,  $\lambda$  and the  
704 relative casualty rate,  $D_r$  under different  $\sigma_{PA}$  and combinations of  
705 parameters related to the increments of  $\alpha$  (i.e.,  $\chi_{FN}$ ,  $\chi_{FP}$ ,  $\chi_{FN} - \chi_{FP}$ , and  $\chi_{TP}$ ). (d-f) Same as (a-c) but for time-averaged  $\alpha$ . (g-i) The relationship between  
706 the warning threshold,  $\lambda$ , and the false warning ratio,  $FWR$ , and the missed  
707 event ratio,  $MER$ , under different  $\sigma_{PA}$ . Each dot shows the result of the  
708 individual Monte Carlo simulation  
709

710 In terms of the effects of the forecasting variance and the tolerance levels of the  
711 failed warnings on the determination of warning threshold as shown in **Figure 911**, the  
712 warning threshold should be decreased if people have a lower tolerance level for the  
713 missed events, and vice versa. And compared to the missed events, the people's low  
714 tolerance levels for the false warnings are less conducive to the effectiveness of flash  
715 flood warnings. These findings are consistent with the results in **Figure 810**.  
716 Furthermore, we find that the difference in the optimal warning thresholds of these  
717 colored curves decreases as the forecasting variance increases as shown in **Figure**

718 **9a11a-Figure 9e11c.** As discussed in the last paragraph of section 4.2, the curve  
719 becomes narrower as the forecasting variance increases. If the width of the curves  
720 decreases, the difference between their optimal warning thresholds will also decrease.  
721 Therefore, as the forecasting variance increases, the difference in the optimal warning  
722 thresholds of these curves will decrease, and the adjustment space for the warning  
723 threshold based on the people's tolerance levels will also decrease.

724 If the green curve represents the result of the baseline scenario where both  $\chi_{FN}$   
725  $\chi_{FN}$  and  $\chi_{FP}$  equal 0.1, increment of the values of  $\chi_{FN}$  and  $\chi_{FP}$  (i.e.,  
726 lowering tolerance levels for the missed events and the false warnings) will result in a  
727 series of curves, and these curves will be enveloped by the green curve in **Figure 911**.  
728 Therefore, only when the green curve is high enough, can the relative casualty rate of  
729 this series of curves be low enough, and the effectiveness of flash flood warnings be  
730 sufficiently improved. And only when the green curve is wide enough, can the  
731 difference in the optimal warning threshold for this series of curves be large enough,  
732 and there can be enough room for adjustment the warning threshold. In summary, by  
733 increasing the height and width of the green curve, the adjustable room for the warning  
734 threshold will be larged and the effectiveness of flash flood warnings will be improved.  
735 As the forecasting accuracy increases, the green curve becomes higher. And as the  
736 forecasting variance decreases, the green curve becomes wider. Therefore, under the  
737 premise of improving the forecasting skills (i.e., increasing forecasting accuracy and  
738 decreasing forecasting variance), adjusting the warning threshold based on the people's  
739 tolerance levels of the failed warnings is one of the ways to improve the effectiveness  
740 of flash flood warnings.



741  
 742 **Figure 911.** (a-c) The relationship between the warning threshold,  $\lambda$  and the  
 743 relative casualty rate,  $D_r$ , under different  $\mu_{PP}$  and combinations of  
 744 parameters related to the increments of  $\alpha$  (i.e.,  $\chi_{FN}$ ,  $\chi_{FP}$ ,  $\chi_{FN} \wedge \chi_{FP}$ , and  $\chi_{TP}$ ). (d-f) Same as (a-c) but for time-averaged  $\alpha$ . (g-i) The relationship between  
 745 the warning threshold,  $\lambda$ , and the false warning ratio,  $FWR$ , and the missed  
 746 event ratio,  $MER$ , under different  $\mu_{PP}$ . Each dot shows the result of the  
 747 individual Monte Carlo simulation.

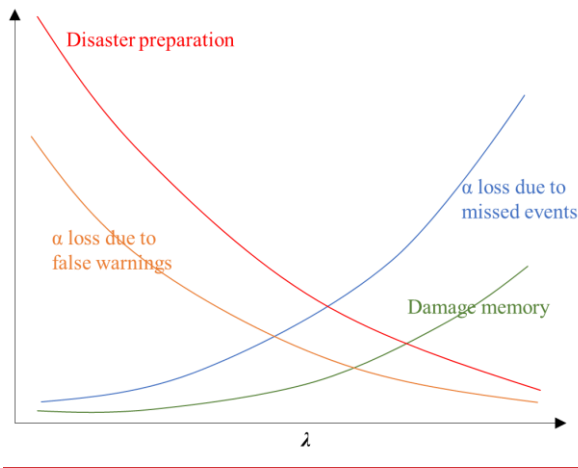
设置了格式: 字体: Times New Roman, 小四

749 **4.4. Implication and limitations**

750 Although the simulation results have deepened our understanding of the warning  
 751 threshold determination, especially the impact of forecasting skills and people's  
 752 tolerance levels of the failed warnings on the warning threshold determination, the  
 753 simulation results should be carefully interpreted due to the assumptions underlying the  
 754 simulation method. As highlighted in the simulation results, the warning threshold  
 755 should be appropriately determined due to the trade-off between multiple factors  
 756 affecting the warning threshold (see Figure 12). Specifically, as the warning threshold



757 increases, the number of missed events and the loss of  $\alpha$  due to missed events will  
 758 increase. And as the missed events increase, the level of disaster preparedness will  
 759 decrease. The loss of  $\alpha$  and the low level of disaster preparedness are not conducive  
 760 to reducing disaster damage. However, as the warning threshold increases, the number  
 761 of false warnings and the loss of  $\alpha$  due to false warnings will decrease, which is  
 762 conductive to reducing disaster damage. Therefore, there is a trade-off in the warning  
 763 threshold determination. However, it has been assumed that the experience of warnings  
 764 (i.e., the success or failure of past warnings) only affects people's trust levels in  
 765 warnings (i.e.,  $\alpha$  ). Actually, the experience of warnings can also affect people's  
 766 attitudes and behaviors towards flash floods. Specifically, the dangerous experiences  
 767 on the property/life losses can form deep flash flood memories. The damage memories  
 768 make people more inclined to evacuate after receiving warnings (Cuite et al., 2017;  
 769 Morss et al., 2018). The higher the warning threshold, the more missed events and  
 770 dangerous experiences there will be, and people's damage memories will be more  
 771 profound. The profound damage memories increase people's evacuation intention and  
 772 reducing disaster damage. Therefore, if combined with the dynamism of human  
 773 behaviors, there still be a trade-off of the warning threshold determination but the  
 774 optimal warning threshold will increase.



775  
 776 **Figure 12.** A schematic diagram that illustrates the trade-off in the warning threshold  
 777 determination

778 The development of the ABM is the core of the simulation flow. The simulation  
 779 results based on the ABM show that there is a monotonic positive relationship between

780  $\alpha$  and casualty rate (see **Figure 7**). The rationale behind the monotonic relationship is  
781 that the higher the value of  $\alpha$ , the more likely a person is to evacuate after receiving a  
782 warning. If someone has evacuated, he/she will lead more people to evacuate, because  
783 neighbor behavior is an important information source for a person to make evacuation  
784 decisions. The developed ABM generalizes these two information sources (i.e., warning  
785 information and neighbor behavior) to simulate the processes of people's evacuation  
786 decision making. However, environmental cue (e.g., rainfall condition) is also an  
787 information source (Lindell et al., 2019). The monotonic positive correlation  
788 relationship between  $\alpha$  and casualty rate may no longer hold true if the environmental  
789 cue is incorporated in the ABM. For example, if there is a flash flood disaster but no  
790 warning is issued, our ABM assumes that no one will evacuate. In fact, if people  
791 observe the rainfall that may lead to flash flood disasters, they will evacuate even if no  
792 warning is issued. The high trust levels in warnings ( $\alpha$ ) may have suppressed their  
793 evacuation intention, leading to a higher casualty rate instead. If the monotonic positive  
794 correlation relationship between  $\alpha$  and casualty rate no longer holds true, the curve  
795 shape in **Figure 8** will no longer be unimodal, and the determination of the optimal  
796 warning threshold will become more complex.

797 The ABM was applied to Liulin Town where residences are located along Lang  
798 River and listed as high-risk and relatively high-risk areas. If there is a flash flood  
799 disaster, the whole town along the river is likely to be submerged and all the people are  
800 required to evacuate. Therefore, the modeling region with an area of 0.28 km<sup>2</sup> is set as  
801 a whole to receive forecasting and warnings. However, if study region is large and  
802 terrain is complex, the study region needs to be divided into multiple sub-regions and  
803 then modeled by the ABM accordingly. For each sub-region, forecasting and warnings  
804 also need to be produced and issued separately. However, in real world, there is usually  
805 a lack of clarity of the sub-region impact of some of the warnings owing to the limitation  
806 of forecasting skills. Forecasting and warning often only target a certain region and are  
807 difficult to distinguish the different degrees of impact within that region (Roberts et al.,  
808 2022). Given a unified forecast and warning for a region, the sub-region along river or  
809 at high-risk areas is prone to missed events, while the sub-region located on a high  
810 ground is prone to false warnings. If it is difficult to improve forecasting skills,  
811 modifying people's tolerance levels of the failed warnings will become one of the ways  
812 to improve the effectiveness of warnings. For example, education or risk

813 communication can be conducted to inform residents of the background and production  
814 process of warning information, allowing them to understand the reasons for false  
815 warnings and missed events, as well as the obstacles to eliminate these issues.  
816 Implementing targeted education or risk communication based on geographical location  
817 to adjust people's tolerance for corresponding types of failed warnings can compensate  
818 for the lack of accuracy in forecasting and warning.

819 It is a tough work to verify the hydrodynamic simulation and people's evacuation  
820 process simulation in small watersheds due to the difficulty in collecting data. The field  
821 flood survey was used to verify the water depth simulated by HEC-RAS. The flood  
822 survey showed that the flood depth of high-rise houses was 1.75 m, while that of houses  
823 with low terrain was 3.85 m in the 8.12 event (Shaojun et al., 2022). The survey results  
824 are roughly consistent with our simulation. In further studies, technologies such as  
825 unmanned aerial vehicle and radar can be used to obtain high-precision inundation data,  
826 and the simulation results can be finely verified based on the inundation data. For the  
827 verification of the evacuation processes simulated by the social sub-module in the ABM,  
828 indirect verification was conducted by investigating and simulating people's evacuation  
829 intention. To directly verifying the evacuation process simulation, milling time can be  
830 surveyed and then converted into data on the evacuation processes in further studies.  
831 Based on the data, the parameters of the social sub-module in the ABM can be  
832 calibrated and verified.

## 833 **5. Conclusions**

834 A method has been proposed to determine the warning threshold for minimizing  
835 casualties based on the people's response process simulation. A process-based ABM  
836 was developed to simulate people's response processes to flash flood warnings. A  
837 simulation chain of "rainstorm probability forecasting - decision on issuing warnings -  
838 warning response processes" was conducted to determine the warning threshold based  
839 on the ABM. The main conclusions are as follows.

840 The casualty rate is jointly controlled by the warning information source and  
841 precipitation. If the people's trust levels in official warnings are below a certain  
842 threshold, precipitation is the dominant factor in controlling the casualty rate. If the  
843 people have a similar level of trust in official warnings and neighbor behaviors, the  
844 credibility of the warning information source is the dominant factor in controlling the  
845 casualty rate.

846 The warning threshold has been determined under different forecasting skills for  
847 minimizing casualties. The lower the forecasting accuracy, the higher the optimal  
848 warning threshold. And the larger the forecasting variance or the variance of the  
849 forecasting variance, the higher (lower) the optimal warning threshold for high (low)  
850 forecasting accuracy. Furthermore, the impact pattern of forecasting skills on the shape  
851 of the relationship curve between the relative casualty rate and the warning threshold  
852 has been revealed: the curve becomes higher as the forecasting accuracy increases, and  
853 the curve becomes narrower as the forecasting variance or the variance of the  
854 forecasting variance increases.

855 The warning threshold has been determined under different forecasting skills and  
856 tolerance levels of the failed warnings for minimizing casualties. The warning threshold  
857 should be decreased (increased) if people have a lower tolerance level for the missed  
858 events (the false warnings). However, if the forecasting accuracy is low and the  
859 forecasting variance is large, the space for adjusting the warning threshold is limited,  
860 and no matter how the warning threshold is adjusted, the casualty rate remains at a high  
861 level, and the effectiveness of flash flood warnings is limited. Therefore, under the  
862 premise of improving the forecasting skills, adjusting the warning threshold based on  
863 the people's tolerance levels of the failed warnings is one of the ways to improve the  
864 effectiveness of flash flood warnings.

865 ~~Although our study provides valuable insights into the determination of warning~~  
866 ~~threshold for minimizing casualties, it should be noted that there are some assumptions~~  
867 ~~underlying the simulation method. The parameters of ABM were assumed to be time~~  
868 ~~invariant except for  $\alpha$ . Updating the values of these parameters based on past warning~~  
869 ~~outcomes will provide more information for determining the warning threshold. The~~  
870 ~~hyetograph was selected as the measured rainfall process of the 8.12 event. More~~  
871 ~~uneven hyetographs should be taken in the flash flood simulation, and the impact of~~  
872 ~~hyetograph on the warning threshold determination can be explored in further research.~~  
873 ~~The casualty rate caused by pluvial floods varies with different spatial distribution of~~  
874 ~~rainfall. The people's trust levels in the warnings were assumed to be only affected by~~  
875 ~~the past warning outcomes. There are other factors (e.g., social education and~~  
876 ~~government authority) that should be incorporate into the estimation of the people's~~  
877 ~~trust levels. Therefore, there are still works can be done in the future.~~

878 **Code availability**

879 The code that supports the findings of this study is available from the  
880 corresponding author upon reasonable request.

881 **Date availability**

882 Data will be made available on request.

883 **Author contribution**

884 Ruikang Zhang: Conceptualization, Formal analysis, Methodology, Writing –  
885 original draft, Visualization, Funding acquisition. Dedi Liu: Conceptualization, Data  
886 curation, Formal analysis, Funding acquisition, Methodology, Supervision, Writing -  
887 review & editing. Lihua Xiong: Project administration, Supervision. Jie Chen: Data  
888 support, Methodology, Writing - review & editing. Hua Chen: Validation, Writing -  
889 review & editing, Supervision. Jiabo Yin: Validation, Writing - review & editing. All  
890 authors contributed to the interpretation of the results and to the text.

891 **Competing interests**

892 The authors declare that they have no conflict of interest.

893 **Disclaimer**

894 Publisher's note: Copernicus Publications remains neutral with regard to  
895 jurisdictional claims in published maps and institutional affiliations.

896 **Acknowledgments**

897 The authors gratefully acknowledge the financial support from National Key  
898 Research and Development Project of China (2022YFC3202803), the National Natural  
899 Science Foundation of China (52379022), and the Open Innovation Foundation funded  
900 by ChangJiang Survey, Planning, Design and Research Co., Ltd (CX2021K04).

901

设置了格式

## References:

- 902  
903 Ambühl, J.: Customer oriented warning systems, *Veröffentlichung—MeteoSchweiz*  
904 *Nr. VERÖFFENTLICHUNG METEOSCHWEIZ NR.* 84, 1-86, 2010.
- 905 Anshuka, A., van Ogtrop, F. F., Sanderson, D., and Leao, S. Z.: A systematic review of agent-based  
906 model for flood risk management and assessment using the ODD protocol, *Nat. Hazards*, 112, 2739-  
907 2771, <https://doi.org/10.1007/s11069-022-05286-y>, 2022-2022.
- 908 Bodoque, J. M., Diez-Herrero, A., Amerigo, M., Garcia, J. A., and Olcina, J.: Enhancing flash flood risk  
909 perception and awareness of mitigation actions through risk communication: A pre-post survey design,  
910 *J. Hydrol.*, 568, 769-779, <https://doi.org/10.1016/j.jhydrol.2018.11.007>, 2019-2019.
- 911 Boelee, L., Lumbroso, D. M., Samuels, P. G., and Cloke, H. L.: Estimation of uncertainty in flood  
912 forecasts-A comparison of methods, *J. Flood Risk Manag.*, 12, e12516, <https://doi.org/10.1111/jfr3.12516>,  
913 2019-2019.
- 914 Borga, M., Comiti, F., Ruin, I., and Marra, F.: Forensic analysis of flash flood response, *Wiley Interdiscip.*  
915 *Rev.-WIREs Water*, 6, e1338, <https://doi.org/10.1002/wat2.1338>, 2019.
- 916 Brazdova, M., and Riha, J.: A simple model for the estimation of the number of fatalities due to floods  
917 in central Europe, *Nat. Hazards Earth Syst. Sci.*, 14, 1663-1676, [https://doi.org/10.5194/nhess-14-1663-](https://doi.org/10.5194/nhess-14-1663-2014)  
918 [2014](https://doi.org/10.5194/nhess-14-1663-2014), 2014.
- 919 Cheng, W.: A review of rainfall thresholds for triggering flash floods, *Advances in Water*  
920 *Science-ADVANCES IN WATER SCIENCE*, 24, 901-908, 2013.
- 921 Coccia, G., and Todini, E.: Recent developments in predictive uncertainty assessment based on the model  
922 conditional processor approach, *Hydrol. Earth Syst. Sci.*, 15, 3253-3274, [https://doi.org/10.5194/hess-15-](https://doi.org/10.5194/hess-15-3253-2011)  
923 [3253-2011](https://doi.org/10.5194/hess-15-3253-2011), 2011-2011.
- 924 Collier, C. G.: Flash flood forecasting: What are the limits of predictability? *Q. J. R. Meteorol. Soc.*, 133,  
925 3-23, <https://doi.org/10.1002/qj.29>, 2007.
- 926 Confalonieri, R., Bellocchi, G., Bregaglio, S., Donatelli, M., and Acutis, M.: Comparison of sensitivity  
927 analysis techniques: A case study with the rice model WARM, *Ecol. Model.*, 221, 1897-1906,  
928 <https://doi.org/10.1016/j.ecolmodel.2010.04.021>, 2010-2010.
- 929 Cools, J., Innocenti, D., and O'Brien, S.: Lessons from flood early warning systems, *Environ. Sci. Policy*,  
930 58, 117-122, <https://doi.org/10.1016/j.envsci.2016.01.006>, 2016-2016.
- 931 Creutin, J. D., Borga, M., Lutoff, C., Scolobig, A., Ruin, I., and Créton-Cazanave, L.: Catchment  
932 dynamics and social response during flash floods: the potential of radar rainfall monitoring for warning  
933 procedures, *Meteorol. Appl.*, 16, 115-125, 2009.
- 934 Cuite, C. L., Shwom, R. L., Hallman, W. K., Morss, R. E., and Demuth, J. L.: Improving coastal storm  
935 evacuation messages, *Weather Clim. Soc.*, 9, 155-170, 2017.
- 936 Du, E., Cai, X., Sun, Z., and Minsker, B.: Exploring the Role of Social Media social media and  
937 Individual Behaviors individual behaviors in Flood Evacuation Processes: An Agent Based Modeling  
938 Approach flood evacuation processes: an agent-based modeling approach, *Water Resour. Res.*, 53, 9164-  
939 9180, <https://doi.org/10.1002/2017WR021192>, 2017-2017.
- 940 Du, E., Wu, F., Jiang, H., Guo, N. L., Tian, Y., and Zheng, C. M.: Development of an integrated socio-  
941 hydrological modeling framework for assessing the impacts of shelter location arrangement and human  
942 behaviors on flood evacuation processes, *Hydrol. Earth Syst. Sci.*, 27, 1607-1626, 2023.
- 943 Duc Anh, D., Kim, D., Kim, S., and Park, J.: Determination of flood-inducing rainfall and runoff for  
944 highly urbanized area based on high-resolution radar-gauge composite rainfall data and flooded area GIS  
945 data, *J. Hydrol.*, 584, 124704, <https://doi.org/10.1016/j.jhydrol.2020.124704>, 2020-2020.
- 946 Han, S. S., and Coulibaly, P.: Bayesian flood forecasting methods: A review, *J. Hydrol.*, 551, 340-351,  
947 <https://doi.org/10.1016/j.jhydrol.2017.06.004>, 2017-2017.
- 948 Hicks, F. E., and Peacock, T.: Suitability of HEC-RAS for Flood Forecasting, *Canadian Water Resources*  
949 *Journal / Revue canadienne des ressources hydriques* flood forecasting, *CANADIAN WATER*  
950 *RESOURCES JOURNAL / REVUE CANADIENNE DES RESSOURCES HYDRIQUES*, 30, 159-174,  
951 <https://doi.org/10.4296/ewrj3002159>, 2005.
- 952 Janssen, M. A., and Ostrom, E.: Empirically based, agent-based models, *Ecol. Soc.*, 11, 37, 2006.
- 953 Jauernic, S. T., and Van den Broeke, M. S.: Tornado Warning Response warning response and  
954 Perceptions perceptions among Undergraduates undergraduates in Nebraska, *Weather Clim. Soc.*, 9, 125-  
955 139, <https://doi.org/10.1175/WCAS-D-16-0031.1>, 2017.
- 956 Ke, Q., Tian, X., Bricker, J., Tian, Z., Guan, G., Cai, H., Huang, X., Yang, H., and Liu, J.: Urban pluvial  
957 flooding prediction by machine learning approaches-a case study of Shenzhen city, China, *Adv. Water*  
958 *Resour.*, 145, 103719, <https://doi.org/10.1016/j.advwatres.2020.103719>, 2020-2020.
- 959 Krzysztofowicz, R.: The case for probabilistic forecasting in hydrology, *J. Hydrol.*, 249, 2-9,  
960 [https://doi.org/10.1016/S0022-1694\(01\)00420-6](https://doi.org/10.1016/S0022-1694(01)00420-6), 2001-2001.

961 LeClerc, J., and Joslyn, S.: The ~~Cry Wolf Effect~~cry wolf effect and ~~Weather-Related Decision~~  
 962 ~~Making~~weather-related decision making, Risk Anal., 35, 385-395, <https://doi.org/10.1111/risa.12336>,  
 963 2015.  
 964 Lei, X., Wang, H., Liao, W., Yang, M., and Gui, Z.: Advances in hydro-meteorological forecast under  
 965 changing environment, J. Hydraul. Eng. ~~ASCE~~, 49, 9-18, 2018.  
 966 Lim, J. R., Liu, B. F., and Egnoto, M.: ~~Cry Wolf Effect? Evaluating~~wolf effect? evaluating the  
 967 ~~Impact~~impact of ~~False Alarms~~false alarms on ~~Public Responses~~public responses to ~~Tornado~~  
 968 ~~Alerts~~tornado alerts in the ~~Southeastern~~southeastern United States, Weather Clim. Soc., 11, 549-563,  
 969 <https://doi.org/10.1175/WCAS-D-18-0080.1> 2019.  
 970 ~~Lindell, M. K., Arlikatti, S., and Huang, S. K.: Immediate behavioral response to the June 17, 2013 flash~~  
 971 ~~floods in Uttarakhand, North India. Int. J. Disaster Risk Reduct., 34, 129-146, 2019.~~  
 972 Lo, S. M., Fang, Z., Lin, P., and Zhi, G. S.: An evacuation model: the SGEM package, Fire Saf. J., 39,  
 973 169-190, <https://doi.org/10.1016/j.firesaf.2003.10.003>, 2004, 2004.  
 974 ~~Maidment, D. R.: CONCEPTUAL FRAMEWORK FOR THE NATIONAL FLOOD~~  
 975 ~~INTEROPERABILITY EXPERIMENT: Conceptual framework for the national flood interoperability~~  
 976 ~~experiment, J. Am. Water Resour. Assoc., 53, 245-257, https://doi.org/10.1111/1752-1688.12474, 2017.~~  
 977 Mileti, D. S.: Factors ~~Related~~related to ~~Flood Warning Response~~, in: ~~Research Workshop on the~~  
 978 ~~Hydrometeorology, Impacts, flood warning response, 1-17, 1995~~  
 979 ~~Morss, R. E., Cuite, C. L., Demuth, J. L., Hallman, W. K., and Management~~Shwom, R. L.: Is storm surge  
 980 scary? The influence of Extreme Floods, Perugia (Italy), 1995hazard, impact, and fear-based messages  
 981 and individual differences on responses to hurricane risks in the USA, Int. J. Disaster Risk Reduct., 30,  
 982 44-58, 2018.  
 983 Oakley, J. E., and O'Hagan, A.: Probabilistic sensitivity analysis of complex models: a Bayesian  
 984 approach, J. R. Stat. Soc. Ser. B-Stat. Methodol., 66, 751-769, [https://doi.org/10.1111/j.1467-](https://doi.org/10.1111/j.1467-9868.2004.05304.x)  
 985 [9868.2004.05304.x](https://doi.org/10.1111/j.1467-9868.2004.05304.x), 2004, 2004.  
 986 O'Hagan, A.: Bayesian analysis of computer code outputs: A tutorial, Reliab. Eng. Syst. Saf., 91, 1290-  
 987 1300, <https://doi.org/10.1016/j.res.2005.11.025>, 2006.  
 988 Oleyiblo, J. O., and Li, Z.: Application of HEC-HMS for flood forecasting in Misai and Wan'an  
 989 catchments in China, Water Sci. Eng., 3, 14-22, [https://doi.org/10.3882/j.issn.1674-](https://doi.org/10.3882/j.issn.1674-2370.2010.01.002)  
 990 [2370.2010.01.002](https://doi.org/10.3882/j.issn.1674-2370.2010.01.002), 2010, 2010.  
 991 ~~Papagiannaki, K., Petrucci, O., Diakakis, M., Kotroni, V., Aceto, L., Bianchi, C., Brázdil, R., Gelabert,~~  
 992 ~~M. G., Inbar, M., Kahraman, A., Kiliç, Ö., Krahn, A., Kreibich, H., Llasat, M. C., Llasat-Botija, M.,~~  
 993 ~~Macdonald, N., de Brito, M. M., Mercuri, M., Pereira, S., Rehor, J., Geli, J. R., Salvati, P., Vinet, F., and~~  
 994 ~~Zêzere, J. L.: Developing a large-scale dataset of flood fatalities for territories in the Euro-Mediterranean~~  
 995 ~~region, FFEM-DB, Sci. Data, 9, 166, 2022.~~  
 996 Parker, D. J., Priest, S. J., and Tapsell, S. M.: Understanding and enhancing the public's behavioural  
 997 response to flood warning information, Meteorol. Appl., 16, 103-114, <https://doi.org/10.1002/met.119>,  
 998 2009.  
 999 ~~Penning-Rowsell, E., Floyd, P., Ramsbottom, D., and Surendran, S.: Estimating injury and loss of life in~~  
 1000 ~~floods: A deterministic framework, Nat. Hazards, 36, 43-64, 2005.~~  
 1001 ~~Petrucci, O.: Review article: Factors leading to the occurrence of flood fatalities: a systematic review of~~  
 1002 ~~research papers published between 2010 and 2020, Nat. Hazards Earth Syst. Sci., 22, 71-83, 2022.~~  
 1003 ~~Petrucci, O., Aceto, L., Bianchi, C., Bigot, V., Brázdil, R., Pereira, S., Kahraman, A., Kiliç, Ö., Kotroni,~~  
 1004 ~~V., Llasat, M. C., Llasat-Botija, M., Papagiannaki, K., Pasqua, A. A., Rehor, J., Geli, J. R., Salvati, P.,~~  
 1005 ~~Vinet, F., and Zêzere, J. L.: Flood Fatalities in Europe, 1980-2018: Variability, Features, and Lessons to~~  
 1006 ~~Learn, Water, 11, 1682, 2019.~~  
 1007 ~~Potter, S., Harrison, S., and Krefit, P.: The Benefits and Challenges of Implementing Impact-Based Severe~~  
 1008 ~~Weather Warning Systems: Perspectives of Weather, Flood, and Emergency Management~~  
 1009 ~~Personnel~~benefits and challenges of implementing impact-based severe weather warning systems:  
 1010 perspectives of weather, flood, and emergency management personnel, Weather Clim. Soc., 13, 303-314,  
 1011 <https://doi.org/10.1175/WCAS-D-20-0110.1>, 2021.  
 1012 Ramos Filho, G. M., Rabelo Coelho, V. H., Freitas, E. D. S., Xuan, Y., and Neves Almeida, C. S.: An  
 1013 improved rainfall-threshold approach for robust prediction and warning of flood and flash flood hazards,  
 1014 Nat. Hazards, 105, 2409-2429, <https://doi.org/10.1007/s11069-020-04405-x>, 2021.  
 1015 Ripberger, J. T., Silva, C. L., Jenkins-Smith, H. C., Carlson, D. E., James, M., and Herron, K. G.: ~~False~~  
 1016 ~~Alarms~~alarms and ~~Missed Events: The Impact~~missed events: the impact and ~~Origins~~origins of ~~Perceived~~  
 1017 ~~Inaccuracy~~perceived inaccuracy in ~~Tornado Warning Systems~~tornado warning systems, Risk Anal., 35,  
 1018 44-56, <https://doi.org/10.1111/risa.12262>, 2015.  
 1019 ~~Roberts, T., Seymour, V., Brooks, K., Thompson, R., Petrokofsky, C., O'Connell, E., and Landeg, O.:~~  
 1020 ~~Stakeholder perspectives on extreme hot and cold weather alerts in England and the proposed move~~

1021 [towards an impact-based approach, Environ. Sci. Policy, 136, 467-475, 2022.](#)

1022 Roulston, M. S., and Smith, L. A.: The Boy who Cried Wolf revisited: The impact of false alarm

1023 intolerance on cost-loss scenarios, *Weather Forecast.*, 19, 391-397, [https://doi.org/10.1175/1520-](https://doi.org/10.1175/1520-0434(2004)019<0391:TBWCWR>2.0.CO;2)

1024 [0434\(2004\)019<0391:TBWCWR>2.0.CO;2, 2004-2004.](https://doi.org/10.1175/1520-0434(2004)019<0391:TBWCWR>2.0.CO;2)

1025 [Salvati, P., Petrucci, O., Rossi, M., Bianchi, C., Pasqua, A. A., and Guzzetti, F.: Gender, age and](#)

1026 [circumstances analysis of flood and landslide fatalities in Italy, Sci. Total Environ., 610, 867-879, 2018.](#)

1027 Sawada, Y., Kanai, R., and Kotani, H.: Impact of cry wolf effects on social preparedness and the

1028 efficiency of flood early warning systems, *Hydrol. Earth Syst. Sci.*, 26, 4265-4278,

1029 [https://doi.org/10.5194/hess-26-4265-2022, 2022-2022.](https://doi.org/10.5194/hess-26-4265-2022)

1030 Shanghai Meteorological Bureau: Rainstorm warning signal, 2019

1031 [Shaojun, X., Yangsheng, J., Hao, J., Oiuju, L., Qi, X., Yi, L., Jun, Z., Feng, W., and Lingsheng, M.:](#)

1032 [Investigation and reflection on "2021.8.12" flood disaster in Liulin Town, Sui County, Hubei Province,](#)

1033 [China Flood & Drought Management, 32, 54-58, 2022.](#)

1034 [Simmons, K. M., and Sutter, D.: False Alarms, Tornado Warnings, and Tornado Casualtiesalarms,](#)

1035 [tornado warnings, and tornado casualties, Weather Clim. Soc., 1, 38-53,](#)

1036 [https://doi.org/10.1175/2009WCAS1005.1, 2009.](https://doi.org/10.1175/2009WCAS1005.1)

1037 Sivapalan, M., and Bloeschl, G.: Time scale interactions and the coevolution of humans and water, *Water*

1038 *Resour. Res.*, 51, 6988-7022, [https://doi.org/10.1002/2015WR017896, 2015.](https://doi.org/10.1002/2015WR017896)

1039 Slater, L., Villarini, G., Archfield, S., Faulkner, D., Lamb, R., Khouakhi, A., and Yin, J.: Global

1040 [Changeschanges in 20-Yearyear, 50-Yearyear, and 100-Year River Floodsyear river floods,](#) *Geophys.*

1041 *Res. Lett.*, 48, e2020GL091824, [https://doi.org/10.1029/2020GL091824, 2021.](https://doi.org/10.1029/2020GL091824)

1042 [Spitalar, M., Gourley, J. J., Lutoff, C., Kirstetter, P. E., Brilly, M., and Carr, N.: Analysis of flash flood](#)

1043 [parameters and human impacts in the US from 2006 to 2012, J. Hydrol., 519, 863-870, 2014.](#)

1044 [Takahashi, S., Endoh, K., and Muro, Z. I.: Experimental study on people's safety against overtopping](#)

1045 [waves on breakwaters, Report on the Port and Harbour Institute, 34, 4-31, 1992.](#)

1046 [Tekeli, A. E., and Fouli, H.: Reducing False Flood Warnings of TRMM Rain Rates Thresholdsfalse flood](#)

1047 [warnings of trmm rain rates thresholds over Riyadh Citycity, Saudi Arabia by Utilizingutilizing AMSR-](#)

1048 [E Soil Moisture Informationsoil moisture information, Water Resour. Manag., 31, 1243-1256, 2017.](#)

1049 [Terti, G., Ruin, I., Anquetin, S., and Gourley, J. J.: A Situation-Based Analysis of Flash Flood Fatalities](#)

1050 [in the United States, Bull. Amer. Meteorol. Soc., 98, 333-345,](#)

1051 [https://doi.org/https://doi.org/10.1007/s11269-017-1573-1175/BAMS-D-15-00276.1, 2017.](https://doi.org/https://doi.org/10.1007/s11269-017-1573-1175/BAMS-D-15-00276.1)

1052 [Todini, E.: Flood Forecasting and Decision Making in the new Millennium. Where are We? Water](#)

1053 [Resour. Manag., 31, 3111-3129, https://doi.org/10.1007/s11269-017-1693-7, 2017-2017.](#)

1054 [Wang, L., Nie, R. H., Slater, L. J., Xu, Z. H., Guan, D. W., and Yang, Y. F.: Education can improve](#)

1055 [response to flash floods, Science, 377, 1391-1392, https://doi.org/10.1126/science.ade6616, 2022-2022.](#)

1056 [Wang, Z. Q., Huang, J., Wang, H. M., Kang, J. L., and Cao, W. W.: Analysis of Flood Evacuation](#)

1057 [Processflood evacuation process in Vulnerable Communityvulnerable community with Mutual Aid](#)

1058 [Mechanism: An Agent-Based Simulation Frameworkmutual aid mechanism: an agent-based simulation](#)

1059 [framework, INTERNATIONAL JOURNAL OF ENVIRONMENTAL RESEARCH AND PUBLIC](#)

1060 [HEALTH, 17, 560, https://doi.org/10.3390/ijerph17020560, 2020.](#)

1061 [Wei, L.: Extreme heavy rainfall in Liulin Town, Suixian County, Hubei Province has resulted in 21](#)

1062 [deaths and 4 loss-of-contactmissing persons, 2021](#)

1063 [Wu, S., Lei, Y., Yang, S., Cui, P., and Jin, W.: An Agent-Based Approachagent-based approach to](#)

1064 [Integrate Human Dynamics Into Disaster Risk Managementintegrate human dynamics into disaster risk](#)

1065 [management, Front. Earth Sci., 9, 818913, https://doi.org/10.3389/feart.2021.818913, 2022.](#)

1066 [Yang, L. E., Scheffran, J., Suesser, D., Dawson, R., and Chen, Y. D.: Assessment of Flood Lossesflood](#)

1067 [losses with Household Responses: Agent-Based Simulationhousehold responses: agent-based simulation](#)

1068 [in an Urban Catchment Areaurban catchment area, Environ. Model. Assess., 23, 369-388,](#)

1069 [https://doi.org/10.1007/s10666-018-9597-3, 2018.](https://doi.org/10.1007/s10666-018-9597-3)

1070 [Yin, J., Gao, Y., Chen, R., Yu, D., Wilby, R., Wright, N., Ge, Y., Bricker, J., Gong, H., and Guan, M.:](#)

1071 [Flash floods: why are more of them devastating the world's driest regions? Nature, 615, 212-215,](#)

1072 [Young, A., Bhattacharya, B., and Zevenbergen, C.: A rainfall threshold-based approach to early warnings](https://doi.org/10.1038/d41586-023-00626-9, 2023-2023.</a></p>
<p>1073 <a href=)

1074 [in urban data-scarce regions: A case study of pluvial flooding in Alexandria, Egypt, J. Flood Risk Manag.,](#)

1075 [14, e12702, https://doi.org/10.1111/jfr3.12702, 2021.](#)

1076 [Younis, J., Anquetin, S., and Thielen, J.: The benefit of high-resolution operational weather forecasts for](#)

1077 [flash flood warning, Hydrol. Earth Syst. Sci., 12, 1039-1051, https://doi.org/10.5194/hess-12-1039-2008,](#)

1078 [2008-2008.](https://doi.org/10.5194/hess-12-1039-2008)

1079 [Zhai, X., Guo, L., Liu, R., and Zhang, Y.: Rainfall threshold determination for flash flood warning in](#)

1080 [mountainous catchments with consideration of antecedent soil moisture and rainfall pattern, Nat. Hazards,](#)



1081 94, 605-625, <https://doi.org/10.1007/s11069-018-3404-y>, 2018, 2018.  
1082 Zhang, R., Liu, D., Du, E., Xiong, L., Chen, J., and Chen, H.: An agent-based model to simulate human  
1083 responses to flash flood warnings for improving evacuation performance, *J. Hydrol.*, 628, 130452,  
1084 <https://doi.org/https://doi.org/10.1016/j.jhydrol.2023.130452>, 2024.  
1085 Zhuo, L., and Han, D. W.: Agent-based modelling and flood risk management: A compendious literature  
1086 review, *J. Hydrol.*, 591, 125600, <https://doi.org/10.1016/j.jhydrol.2020.125600>, 2020, 2020.  
1087